BRAIN
ORIGINAL ARTICLE

Disease-linked mutations in Munc18-1 deplete synaptic Doc2

Noah Guy Lewis Guiberson, Luca S. Black,† Jillian E. Haller,† Aniv Brukner, Debra Abramov, Saad Ahmad, Yan Xin Xie, Manu Sharma and Jacqueline Burré

†These authors contributed equally to this work.

Heterozygous *de novo* mutations in the neuronal protein Munc18-1/STXBP1 cause syndromic neurological symptoms, including severe epilepsy, intellectual disability, developmental delay, ataxia and tremor, summarized as STXBP1 encephalopathies. Although haploinsufficiency is the prevailing disease mechanism, it remains unclear how the reduction in Munc18-1 levels causes synaptic dysfunction in disease as well as how haploinsufficiency alone can account for the significant heterogeneity among patients in terms of the presence, onset and severity of different symptoms.

Using biochemical and cell biological readouts on mouse brains, cultured mouse neurons and heterologous cells, we found that the synaptic Munc18-1 interactors Doc2A and Doc2B are unstable in the absence of Munc18-1 and aggregate in the presence of disease-causing Munc18-1 mutants. In haploinsufficiency-mimicking heterozygous knockout neurons, we found a reduction in Doc2A/B levels that is further aggravated by the presence of the disease-causing Munc18-1 mutation G544D as well as an impairment in Doc2A/B synaptic targeting in both genotypes. We also demonstrated that overexpression of Doc2A/B partially rescues synaptic dysfunction in heterozygous knockout neurons but not heterozygous knockout neurons expressing G544D Munc18-1.

Our data demonstrate that STXBP1 encephalopathies are not only characterized by the dysfunction of Munc18-1 but also by the dysfunction of the Munc18-1 binding partners Doc2A and Doc2B, and that this dysfunction is exacerbated by the presence of a Munc18-1 missense mutant. These findings may offer a novel explanation for the significant heterogeneity in symptoms observed among STXBP1 encephalopathy patients.

Helen and Robert Appel Alzheimer's Disease Research Institute, Brain and Mind Research Institute, Weill Cornell Medicine, New York, NY 10021, USA

Correspondence to: Noah Guy Lewis Guiberson
Helen and Robert Appel Alzheimer's Disease Research Institute & Brain and Mind Research Institute
Weill Cornell Medicine, 413 East 69th Street, New York, NY 10021, USA
E-mail: nog2008@med.cornell.edu

Correspondence may also be addressed to: Jacqueline Burré
E-mail: jab2058@med.cornell.edu

Keywords: encephalopathy; doc2; Munc18-1; STXBP1; synapse

Received May 31, 2022. Revised November 20, 2023. Accepted January 09, 2024. Advance access publication January 18, 2024

Introduction

Mutations in Munc18-1 (encoded by the *STXBP1* gene) cause a variety of neurodevelopmental disorders known collectively as STXBP1 encephalopathies.[1,2] STXBP1 encephalopathies include severe early-onset epileptic encephalopathies[3-5] as well as non-syndromic epilepsies, atypical Rett syndrome and severe intellectual disability without epilepsy.[6-9] These devastating and often fatal infantile encephalopathies are all characterized by intellectual disability and cerebral dysfunction, and most include epileptic syndromes with eventual cognitive, sensory and/or motor function deterioration.[10-12] In addition, they vary considerably in their age of onset, developmental outcome, aetiology and seizure type[3,11,13] and tend to be refractory to standard antiepileptics.[14,15]

Causative mutations are typically *de novo* and heterozygous and include missense, frameshift, truncation, splice site and partial deletion mutations.[1,2] Many of the mutations result in an unstable protein that aggregates and/or is degraded,[16-18] which led to the proposal of haploinsufficiency as the primary disease mechanism. However, it remains unclear how haploinsufficiency alone can account for different mutations in a single gene, leading to such remarkably variable disease onsets and clinical presentations; why certain types of mutations cause different sets of symptoms/severities; and why some missense mutations cause phenotypes that are more severe than others.[1,2,19]

Munc18-1 belongs to the SEC1/Munc18-like family of proteins, which is essential to secretion in a variety of organisms, including yeast (SEC1),[20] *Caenorhabditis elegans* (UNC-18),[21] zebrafish (Stxbp1),[22] *Drosophila melanogaster* (ROP)[23] and mice (Munc18-1).[24] Munc18-1 is present in the presynapse and interacts with numerous binding partners, including syntaxin-1,[25,26] Doc2A/B,[27] rab3[28] and Mint1/2, to support and regulate synaptic functions.[29] Syntaxin-1 is a SNARE protein that, along with its cognate SNAREs SNAP-25 and VAMP2, enables the fusion of synaptic vesicles with the presynaptic plasma membrane to govern neurotransmitter release into the synaptic cleft. Munc18-1 protects syntaxin-1 from forming ectopic SNARE complexes while trafficking to the cell surface,[30] regulates the formation of SNARE complexes with its cognate binding partners at the synapse[25,31-40] and acts as a template for SNARE complex assembly.[41-44] The interactions between Munc18-1 and its binding partners and the relevance of those interactions to synaptic function are not well understood. Doc2A and Doc2B (double C2 domain proteins)[27] compete with syntaxin-1 to bind to Munc18-1, which may regulate the Munc18-1/syntaxin-1 interaction during vesicle docking.[27] Doc2A/B have been proposed to be calcium sensors for spontaneous neurotransmitter release[45-49] and modulators of synaptic plasticity.[49-51] Other notable Munc18-1 interactors are Mint1 and Mint2 (Munc18-1 interacting proteins), which bind to the Munc18-1/syntaxin-1 complex[29] and may recruit Munc18-1 to the active zone.[52] Munc18-1 also binds to rab3 proteins, a family of synaptic GTPases that function in synaptic vesicle docking.[53-55]

In Munc18-1 knockout mouse brains harvested from embryos at embryonic Day 18 (E18), the levels of syntaxin-1, Doc2A and Doc2B are significantly reduced, indicating that these proteins depend on the abundance of Munc18-1 for their stability, whereas the levels of rab3, Mint1 and Mint2 are unaffected.[56] In Munc18-1 heterozygous knockout mouse brains harvested from E18 embryos, none of these proteins exhibited significantly reduced levels.[56] These findings suggested that disease-causing mutations in Munc18-1 that are predicted to lead to haploinsufficiency are unlikely to affect the levels of Munc18-1 interactors. However, this remains unexplored, and the effect of mutations in Munc18-1 on Munc18-1 effectors is unknown. In addition, Munc18-1 can dimerize,[18] and missense mutants that retain this binding ability destabilize and co-aggregate wild-type (WT) Munc18-1.[18,57] This gain-of-function effect of Munc18-1 missense mutants may not only further reduce functional levels of Munc18-1 into a range that is insufficient to stabilize its binding partners but also exert a direct destabilizing effect on Munc18-1 interactors. Furthermore, different mutations in Munc18-1 may differentially impact Munc18-1 binding partners, which may explain the variability in symptoms and disease outcome.

Current knowledge about the disease mechanisms underlying Munc18-1/STXBP1 encephalopathies is restricted to the primary cause, mutations in Munc18-1, with no understanding of the downstream cascade or effectors. Here, we found that the Munc18-1 interacting proteins Doc2A and Doc2B are additional targets, resulting in reduced levels and reduced solubility, particularly at the neuronal synapse, and contributing to the synaptic deficits observed in these diseases. This is the first study to identify a specific secondary target, the dysfunction of which contributes to the disease phenotypes in Munc18-1/STXBP1 encephalopathies. Beyond stabilizing functional Munc18-1 levels, restoring functional Doc2 levels is therefore a viable therapeutic strategy.

Materials and methods

Mouse strains

The conditional Munc18-1 knockout mouse was kindly donated by Dr Matthijs Verhage (CNCR, The Netherlands). Mice were bred either as homozygous or heterozygous conditional Munc18-1 knockout mice. No inclusion criteria for neuronal cultures were used. We additionally generated constitutive STXBP1 heterozygous knockout mice by crossing floxed STXBP1 mice from the Verhage lab[56] with mice expressing Cre recombinase (Cre) under the constitutive β-actin promoter.[58] Mice were then outcrossed to remove the Cre transgene. Mice were housed under a 12-h light/dark cycle in a temperature-controlled room with free access to water and food. All animal procedures were performed according to National Institutes of Health guidelines and approved by the Committee on Animal Care at Weill Cornell Medicine.

Cell culture and maintenance

HEK293T cells (ATCC) were maintained in Dulbecco's modified Eagle medium (DMEM) with 1% penicillin/streptomycin and 10% bovine serum. Cells were used solely as protein expression systems or to produce lentivirus and were not authenticated or tested for mycoplasma contamination. Mouse cortical neurons were cultured from newborns of either sex. Cortices were dissected in ice-cold Hanks' balanced salt solution (HBSS), dissociated and triturated with a siliconized pipette and plated onto 6 mm poly-L-lysine-coated coverslips (for immunofluorescence) or 24-well plastic dishes. Plating media (MEM supplemented with 5 g/l glucose, 0.2 g/l $NaHCO_3$, 0.1 g/l transferrin, 0.25 g/l insulin, 0.3 g/l L-glutamine and 10% fetal bovine serum (FBS) was replaced with growth media (MEM containing 5 g/l glucose, 0.2 g/l $NaHCO_3$, 0.1 g/l transferrin, 0.3 g/l L-glutamine, 5% FBS, 2% B-27 supplement and 2 μM cytosine arabinoside) 2 days after plating. At 6 days *in vitro* (DIV), neurons were transduced with recombinant lentiviruses expressing myc-tagged Munc18 variants, Cre and/or inactive Cre recombinase (ΔCre; control) or Doc2A and Doc2B. Neurons were harvested or used for experiments as indicated at 13 or 20 DIV.

Expression vectors

Full-length human *Munc18-1b* cDNA was inserted into pCMV5 or the lentiviral vector FUW, containing an N-terminal myc-tag and a two amino acid linker, resulting in the following N-terminal sequence (EQKLISEEDL-GG). Mutant Munc18-1b constructs were generated by site-specific mutagenesis, according to the manufacturer's protocol (Stratagene). Full-length mouse *Doc2A*, mouse *Doc2B*, rat *Mint1*, rat *Mint2* or mouse *rab3* were inserted into pCMV5, containing an N-terminal HA-tag and a four-residue glycine linker, resulting in the following N-terminal sequence (YPYDVPDYA-GGGG). Full-length mouse Doc2A and Doc2B were also generated without an N-terminal epitope tag. pCMV5 syntaxin-1A has been described elsewhere.[59] Expression of neuronal TdTomato was achieved by inserting TdTomato cDNA into a lentiviral vector driving protein expressing via the neuronal synapsin promoter.

Transfection of HEK293T cells

Cells were transfected with cDNA using calcium phosphate produced in-house: 1 h prior to transfection, 25 µM chloroquine in fresh media was added. DNA was incubated for 1 min at room temperature (RT) in 100 mM $CaCl_2$ and 1× HBSS (25 mM HEPES pH 7.05, 140 mM NaCl, and 0.75 mM Na_2HPO_4), and the transfection mix was then slowly added to the cells. Medium was replaced with fresh medium after 6 h. Cells were harvested or used for experiments as indicated 2 days after transfection. For lentivirus production, HEK293T cells were co-transfected with equimolar amounts of lentiviral vectors FUW containing myc-tagged Munc18-1, FUW containing Doc2A or Doc2B or FSW containing TdTomato, and pMD2-G-VSVg (Addgene #12259), pMDLg/pRRE (Addgene #12251) and pRSV-Rev (Addgene #12253). Medium containing the viral particles was collected 48 h later and centrifuged for 5 min at 500g_{av} to remove cellular debris. Viral particles were subsequently concentrated 10-fold by centrifugation.

Total protein levels

Forty-eight hours after transfection of HEK293T or at indicated days after transduction of primary neurons, cells were washed twice in PBS containing 1 mM $MgCl_2$ and solubilized in 2× Laemmli sample buffer containing 30.8 mg/ml dithiothreitol (DTT). Samples were then sonicated and boiled for 20 min at 100°C before separation by sodium dodecyl-sulphate polyacrylamide gel electrophoresis (SDS-PAGE).

Triton X-100 solubilization assay

Cells were washed twice with PBS containing 1 mM $MgCl_2$ and removed from the dish using PBS. Cells were pelleted by centrifugation (5 min at 500g_{av}) and were solubilized in 0.1% Triton X-100 in PBS supplemented with protease inhibitors for 1 h at 4°C under constant agitation. Insoluble material was pelleted by centrifugation (10 min at 13 000g_{av} and 4°C), the Triton X-100 soluble supernatant was transferred to a fresh tube, and the pellet was adjusted to the same volume with PBS. Both fractions were supplemented with 5× Laemmli sample buffer containing 77 mg/ml DTT and sonicated before separating equal volumes by SDS-PAGE.

Limited proteolysis

Cells were washed twice in PBS containing 1 mM $MgCl_2$, lysed by freezing for at least 60 min at –80°C and incubated in the indicated concentrations of trypsin on ice for 5 min. Tryptic digestion was immediately stopped by the addition of 5× Laemmli sample buffer containing 77 mg/ml DTT and boiling for 20 min at 100°C.

Immunocytochemistry

Cells were washed twice with PBS containing 1 mM $MgCl_2$ and fixed with 4% paraformaldehyde in PBS for 20 min at RT. Cells were washed twice with PBS and permeabilized with 0.1% Triton X-100 in PBS for 5 min at RT. After washing twice with PBS, cells were blocked for 20 min with 5% bovine serum albumin (BSA) in PBS. Primary antibody was added in 1% BSA in PBS overnight at 4°C. The next day, cells were washed twice in PBS, blocked for 20 min in 5% BSA in PBS and incubated with secondary antibody and DAPI in 1% BSA in PBS for 1 h at RT in the dark. Cells were washed twice with PBS and were mounted using Fluoromount-G™. Cells were imaged on an Eclipse 80i upright fluorescence microscope (Nikon).

Quantification of aggregates in images of neurons

Images of fixed cortical neuron cultures immunostained with anti-Doc2A/B antibody (N321) and anti-myc antibody were captured blind to the genotype. The percentage of cells with aggregates per field was recorded blind to the genotype. Doc2A/B aggregates were identified as bright Doc2A/B-positive puncta within the cell body, visually distinguishable from diffuse, background Doc2A/B immunofluorescence.

Antibody uptake assay

Cells were equilibrated for 10 min at RT in Krebs-Ringer solution [128 mM NaCl, 25 mM HEPES, 4.8 mM KCl, 1.3 mM $CaCl_2$, 1.2 mM $MgSO_4$, 1.2 mM KH_2/K_2HPO_4 (pH 7.4), 5.6% glucose, pH 7.4]. The medium was then replaced with Krebs-Ringer solution containing 55 mM KCl (and a corresponding reduction in NaCl) for 5 min at RT, with a 1:50 dilution of luminal synaptotagmin-1 antibody. Cells were washed three times for 1 min with Krebs-Ringer solution and fixed with 4% paraformaldehyde in PBS. After washing twice with PBS, cells were permeabilized using 0.1% Triton X-100 in PBS for 5 min and blocked for 20 min with 5% BSA in PBS. An anti-SV2 antibody was added in 1% BSA in PBS overnight at 4°C, and cells were then incubated with secondary antibodies as described above. Neurons were imaged on an Eclipse 80i upright fluorescence microscope (Nikon) at the same fluorescence intensity settings. For each image, a binary mask of the synaptic area was created from the SV2 signal and used to restrict the measurement of Doc2 fluorescence to synapses. The analysis was done in ImageJ (NIH).

Multi-electrode array

Primary neurons were cultured on 48-well CytoView microelectrode array (MEA)™ plates (Axion BioSystems) at one postnatal Day 0 (P0) pup per plate with 2.67 µg/µl laminin. Cells were transduced at 5 DIV with lentiviral vectors. Spontaneous activity was recorded at 14 DIV for 15 min using the Maestro Pro MEA system (Axion BioSystems). Spikes were differentiated from raw signal via a detection threshold established for each electrode of ±6× the standard deviation of the noise (AxIS Navigator software, Axion Biosystems). Electrodes with at least 5 spikes/min were considered active, and electrodes without activity were excluded from analyses. Burst metrics were analysed using the Neural Metric Tool (Axion Biosystems). Bursts were identified as events with a

minimum of five spikes on an individual electrode with a maximum inter-spike interval of 0.1 s. Network bursts were measured with an adaptive algorithm and identified as events with at least 40 spikes across a minimum of 25% of the electrodes within a single well.

SynaptopHluorin assay

Mouse cortical neurons were lentivirally transduced as described above and co-transduced with lentiviral vectors expressing synaptophysin-pHluorin (SypHy) and TdTomato for neuronal identification. Neurons were equilibrated for 10 min at RT in Krebs-Ringer solution. SypHy fluorescence was excited using a 470 nm LED and monitored at ×40 magnification using time-lapse recording with 300-ms intervals on an Eclipse TS2-FL inverted fluorescence microscope (Nikon) equipped with a Zyla Plus sCMOS 4.2 MP camera (Andor). Before the stimulus, we recorded for 10 s to determine the baseline SypHy fluorescence in cells, and exocytosis was then triggered with 55 mM KCl in Krebs-Ringer solution. The change in fluorescence over baseline fluorescence (ΔF/Fi) as a fraction of the maximum possible fluorescence from the entire SypHy pool (by treatment with 50 mM NH_4Cl) was analysed using Elements BR Analysis 5.21.02 Software (Nikon). The regions of interest were selected around the spatially resolved SypHy-positive puncta corresponding to synaptic terminals.

Quantitative immunoblotting

Protein samples were separated by SDS-PAGE and transferred onto nitrocellulose membranes. Blots were blocked in Tris-buffered saline (TBS) containing 0.1% Tween-20 (TBS-T) containing 5% fat-free milk for 30 min at RT. The blocked membrane was incubated overnight in PBS containing 1% BSA, 0.2% NaN_3 and the primary antibody. The blots were then washed twice in TBS-T containing 5% fat-free milk and incubated for 1 h in the same buffer containing secondary antibody at RT. Blots were then washed three times in TBS-T, twice in water and then dried in the dark. Blots were imaged using a LI-COR Odyssey CLx, and images were analysed using ImageStudioLite (LI-COR).

Antibodies

Monoclonal antibodies used were: β-actin (A1978, Sigma), Doc2B (N150/21, BioLegend), GAPDH (sc-32233, Santa Cruz), GFP (632381, Takara Bio Clontech), HA (901503, BioLegend), Munc18-1 (610337, BD Biosciences), myc (9E10, DSHB), Synaptotagmin-1 (105221, Synaptic Systems), SV2 (deposited to the DSHB by Buckley, K.M. (DSHB Hybridoma Product SV2)), syntaxin-1 (HPC1, Santa Cruz), α-tubulin (12G10, DSHB), Tuj-1 (2G10, Santa Cruz) and VAMP2 (3E5, Santa Cruz). Polyclonal antibodies used were: Munc18-1 (610336, BD), Doc2A/B (N321, gift from Dr Thomas Südhof), Doc2A (GTX119085, Genetex; AF7904, R&D), Doc2B (174103, Synaptic Systems), myc (C3956, Sigma) and SV2 (P915, gift from Dr Thomas C. Südhof).

Synaptosome isolation

Synaptosomes were isolated as previously described.[60] Briefly, mouse brains or cultured cortical neurons were homogenized in preparation buffer (5 mM Tris-HCl, 320 mM sucrose, pH 7.4), supplemented with protease inhibitors. The homogenate was centrifuged for 10 min at $1000g_{av}$. The supernatant was collected, and the pellet was resuspended in preparation buffer and recentrifuged. Both supernatants were pooled, and the final pellet was discarded. Discontinuous Percoll gradients were prepared by layering 7.5 ml (200 µl for cultured cortical neurons) supernatant onto three layers of 7.5 ml (200 µl for cultured cortical neurons) Percoll solution (3%, 10% and 23% v/v in 320 mM sucrose, 5 mM Tris-HCl, pH 7.4). After centrifugation for 7 min at $31\,400g_{av}$, fractions containing synaptosomes were collected.

Quantification and statistical analysis

Sample sizes were chosen based on preliminary experiments or similar studies performed in the past. For quantification of immunoblots, a minimum of three independent experiments were performed. To ensure reliable quantification of immunofluorescence microscopy images, images were recorded under the same microscope settings (objective lens and illumination intensity). Merged images were created and analysed using ImageJ (NIH). All data are presented as the mean ± standard error of the mean (SEM) and represent a minimum of three independent experiments. Statistical analyses were performed using Prism 7 Software (GraphPad). For the statistical comparison of groups, either two-tailed Student's *t*-test, one-way ANOVA (followed by Tukey–Kramer's *post hoc* multiple comparisons test) or two-way ANOVA was performed. Formal tests for data normality (Kolmogorov–Smirnov test, Shapiro–Wilk test, D'Agostino–Pearson test and/or Anderson–Darling test) were performed in combination with visual inspection of quantile-quantile (Q-Q) plots. If an abnormal distribution of data was identified, non-parametric tests such as the Mann–Whitney U-test or Kruskal–Wallis test (followed by Dunn's *post hoc* multiple comparisons test) was performed. A value of $P < 0.05$ was considered statistically significant.

Results

Munc18-1 controls the stability of syntaxin-1, Doc2A and Doc2B

The levels of syntaxin-1, Doc2A and Doc2B are significantly reduced in Munc18-1 knockout brains harvested from E18 embryos.[56] To determine whether this relationship between Munc18-1 and syntaxin-1 and Doc2A/B persists in cultured neurons, we analysed cortical neurons from P0 conditional Munc18-1 KO mice (Munc18-1 fl/fl)[61] that were infected with Cre to induce knockout of Munc18-1 or with an inactive version of Cre as control (ΔCre; WT). We observed that the lack of Munc18-1 led to a drastic reduction in the levels of syntaxin-1 and Doc2A/B (Fig. 1A), not only verifying the previously reported results but enabling us to use cultured neurons and their manipulation to assess the effects of different Munc18-1 genotypes on Munc18-1 effectors.

However, Munc18-1 knockout is accompanied by a reduction in neuronal viability,[24,62] and although we did not find changes in the levels of the presynaptic protein VAMP2 (Fig. 1A), arguing against neuron death, the reduction in syntaxin-1 and Doc2 levels was possibly due to changes in neuronal viability or health. We therefore utilized HEK293T cells, which do not express Munc18-1 endogenously, as a reduced system. This enabled us not only to study the relationship between Munc18-1 and its binding partners without indirect effects on protein levels caused by neuronal degeneration but also allowed us tighter control over protein expression levels. In addition, expression in HEK293T cells permitted us to assess the relationship between Munc18-1 and its effectors in the absence of other neuronal protein binding partners. For Doc2A and Doc2B, we pursued a strategy with epitope-tagged and untagged variants,

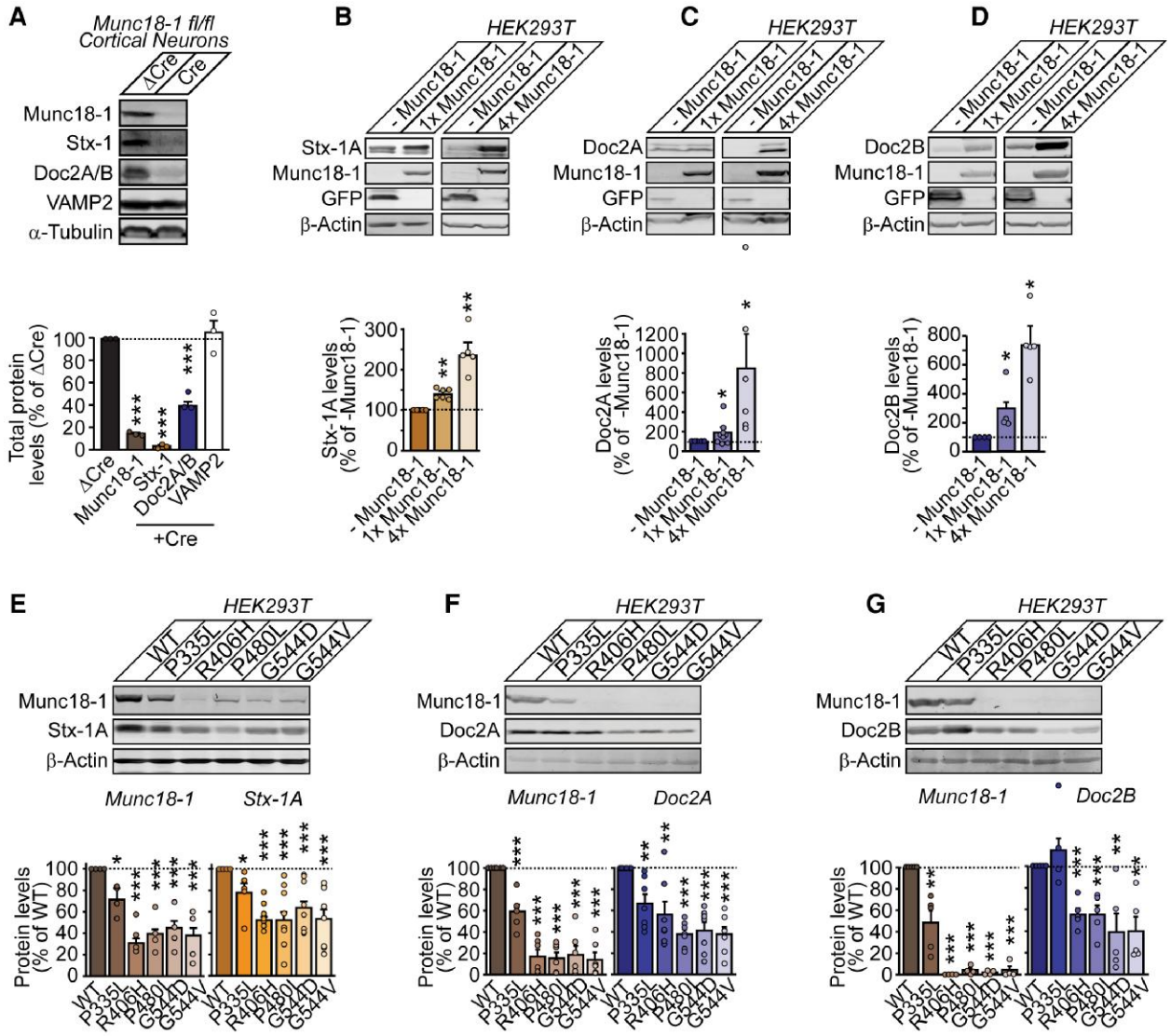

Figure 1 Munc18-1 controls the stability of syntaxin-1, Doc2A and Doc2B. (**A**) Analysis of protein levels in Munc18-1 knockout neurons. Double-floxed (fl/fl) Munc18-1 neurons were transduced at 6 days *in vitro* with lentiviral vectors expressing either Cre recombinase (Cre) or inactive Cre recombinase (ΔCre) as a control. Total protein levels were quantified at 20 days *in vitro* by immunoblotting, normalized to the levels of α-tubulin. Student's *t*-test; ***$P < 0.001$; $n = 3$ independent experiments. Stx-1 = syntaxin-1. (**B–D**) Munc18-1 promotes stability of syntaxin-1A, Doc2A and Doc2B. HEK293T cells were co-transfected with cDNA expressing syntaxin-1A (**B**), HA-tagged Doc2A (**C**) or HA-tagged Doc2B (**D**) and 1- or 4-fold (1× or 4×) amounts of Munc18-1b cDNA or GFP to balance the total amount of DNA. Two days after transfection, protein levels in cell homogenates were analysed by quantitative immunoblotting, normalized to β-actin. Student's *t*-test; *$P < 0.05$, **$P < 0.01$; $n = 4–9$ independent experiments. (**E–G**) Effect of missense mutations in Munc18-1 on the levels of syntaxin-1A, Doc2A and Doc2B. Wild-type (WT) or mutant Munc18-1 was co-expressed with syntaxin-1A (**E**), HA-tagged Doc2A (**F**) or HA-tagged Doc2B (**G**) in HEK293T cells. Two days after transfection, cells were harvested and analysed for total protein levels, normalized to β-actin. One-way ANOVA with Tukey–Kramer *post hoc* test or Mann–Whitney U-test; *$P < 0.05$, **$P < 0.01$, ***$P < 0.001$; $n = 4–7$ independent experiments. Data are presented as mean ± standard error of the mean.

enabling us to test antibodies for their specificity to each isoform (Supplementary Fig. 1). In all subsequent experiments in which an anti-Doc2 antibody was used, we incorporated N321, which recognized both Doc2A and Doc2B (Supplementary Fig. 1).

Data published by our group and other groups suggest that some Munc18-1 interacting proteins depend on the presence of Munc18-1 for stability. To ascertain the relationship between Munc18-1 levels and interactor levels, we first tested whether increasing the Munc18-1 levels stabilizes interactor levels. For this, we expressed increasing amounts of Munc18-1 in HEK293T cells co-expressing one of the Munc18-1 effectors syntaxin-1, Doc2A, Doc2B, rab3, Mint1 or Mint2. Stable effector levels were achieved by balancing the total amount of cDNA with a construct expressing GFP. We observed that Munc18-1 stabilized syntaxin-1, Doc2A and Doc2B levels in a concentration-dependent manner (Fig. 1B–D and Supplementary Fig. 2A and B) but did not affect the levels of rab3, Mint1 or Mint2 (Supplementary Fig. 2C–E). Doc2A and Doc2B were unable to stabilize Munc18-1 (Supplementary Fig. 2F and G), in contrast to syntaxin-1.[63]

Many disease-causing mutations in Munc18-1 result in destabilized Munc18-1 that aggregates and/or is degraded.[5,17,18,57,64] We have previously reported that the Munc18-1 mutants R406H, P480L, G544D and G544V exhibit profoundly reduced protein levels, while the mutant P335L displays an intermediate reduction in

protein levels relative to WT Munc18-1.[18] When we tested the impact of these mutations on Munc18-1's interacting proteins in HEK293T cells co-expressing syntaxin-1, Doc2A, Doc2B, rab3, Mint1 or Mint2, we found that the levels of syntaxin-1, Doc2A and Doc2B were similarly reduced in the presence of mutant Munc18-1, with a ~50% reduction in the presence of Munc18-1 mutants, except for P335L, which caused a milder phenotype (Fig. 1E–G). Conversely, mutant Munc18-1 had no effect on the levels of rab3, Mint1 or Mint2 (Supplementary Fig. 2H–J), in agreement with the findings presented earlier (Fig. 1).

Munc18-1 destabilizes and co-aggregates syntaxin-1, Doc2A and Doc2B in HEK293T cells

Munc18-1 can dimerize[18] and mutant Munc18-1 retains the ability to bind to WT Munc18-1, resulting in the destabilization and co-aggregation of mutant and WT Munc18-1.[18,57] In addition, mutant Munc18-1 co-aggregates α-synuclein,[57] indicating that mutant Munc18-1 may be able to draw other proteins including its binding partners into aggregates as well.

To test this, we used the mild non-ionic detergent Triton X-100 to solubilize transfected HEK293T cell homogenates (Fig. 2A) co-expressing WT or mutant Munc18-1 along with either syntaxin-1, Doc2A, Doc2B, rab3, Mint1 or Mint2. We found that compared with the WT, mutant Munc18-1 was highly insoluble, except for the P335L mutation, confirming our previous findings,[18] and recruited syntaxin-1, Doc2A and Doc2B into the insoluble fraction (Fig. 2B–D and Supplementary Fig. 3A–D), while the solubility of rab3, Mint1 and Mint2 was unaffected (Supplementary Fig. 3E–G).

We then analysed the solubility of Doc2A and Doc2B alone or in the presence of either WT or G544D mutant Munc18-1. We found that in the presence of WT Munc18-1, the solubility of both Doc2A and Doc2B was increased, while the G544D variant reduced the solubility of Doc2A and Doc2B below the solubility of Doc2 alone (Fig. 2E and F). This indicates that the effect of mutant Munc18-1 on the solubility of Doc2A and Doc2B is not merely due to the reduced levels of the mutant but also due to the presence of the mutant itself.

We separately assessed the co-aggregation of Munc18-1 with its effectors under native conditions, in the absence of detergent, using limited proteolysis on HEK293T cells (Fig. 3A). As we have shown previously,[18] Munc18-1 mutants were significantly less susceptible to tryptic digestion than WT Munc18-1, indicating protein misfolding. Strikingly, this reduced solubility in the presence of mutant but not WT Munc18-1 was mimicked by Doc2A and Doc2B (Fig. 3B–G). Interestingly, syntaxin-1 did not exhibit this decreased susceptibility to tryptic digestion in the presence of mutant Munc18-1 (Supplementary Fig. 4A–C), possibly due to the stabilizing effect of over-expressed syntaxin-1 on Munc18-1 mutants.[63] Munc18-1 and syntaxin-1 may also mutually stabilize one another, as evidenced by the reduction of syntaxin-1 levels in the brains of Munc18-1 knockout mice[56] and the reduction of Munc18-1 levels in the brains of syntaxin-1A/B double knockout mice.[65] Similarly, the susceptibility to tryptic digestion of rab3 (Supplementary Fig. 5A–C), Mint1 (Supplementary Fig. 6A–C), Mint2 (Supplementary Fig. 7A–C) and β-actin as the control (Supplementary Fig. 8A–C) was not affected by mutations in Munc18-1.

Munc18-1 mutants cause Doc2A and Doc2B to aggregate and mislocalize in cultured mouse neurons

We demonstrate above that mutations in Munc18-1 do not only affect Munc18-1 levels and solubility but also the levels and solubility of some of its interactors (Figs 1–3). Yet, while the HEK293T cell system has several advantages, these experiments involved overexpression of neuronal proteins in a non-neuronal system. So not only non-physiological levels but also non-physiological subcellular targeting may have impacted our findings. We therefore used cultured cortical neurons from P0 Munc18-1 conditional knockout mice and lentivirally expressed both Cre and either myc-tagged WT or mutant Munc18-1 at endogenous levels.[18] As several studies have already explored the relationship between disease-causing Munc18-1 mutants and syntaxin-1,[5,17,64,66,67] we focused here on Doc2A and Doc2B.

Confirming our findings presented earlier (Fig. 1F and G), the fluorescence intensity of Munc18-1 was markedly reduced in neurons expressing Munc18-1 mutants, particularly in the synaptic and dendro-axonal compartments (Fig. 4A and B). In cells expressing WT Munc18-1, Doc2A/B co-localized with Munc18-1 both in the soma as well as in small puncta extending away from the soma (Fig. 4A and B). Additionally, we observed large Doc2A/B-positive aggregates in the cell bodies of neurons expressing Munc18-1 mutants (Fig. 4A and B).

While the effect of depleted Munc18-1 on Doc2A/B levels has been indicated,[56] the effect on Doc2A/B localization remains unknown. Doc2A/B are cytosolic proteins that are enriched in the presynapse.[68] To confirm that Doc2A/B are neuronal and synaptic and assess whether Munc18-1 mutants alter this localization, we analysed double-floxed Munc18-1 neurons lentivirally expressing ΔCre (WT), Cre (knockout) or Cre + G544D Munc18-1 (G544D). Note that we focused on G544D because this mutant exhibited severe aggregation and impairments in neurotransmitter release in our previous studies[18,63] and multiple different mutations at residue 544 are linked to disease.[1,2] When we analysed the co-localization of Doc2A/B with Tuj-1 (Fig. 4C), a neuron-specific tubulin isoform, or with the integral synaptic vesicle protein SV2, as a presynaptic marker (Fig. 4D), we found that the Doc2A/B puncta that extended away from cell bodies contacted Tuj-1-positive neuronal processes (Fig. 4C) and that Doc2A/B co-localized with SV2 (Fig. 4D). When we quantified Doc2A/B under an SV2 mask, we found that the synaptic levels of Doc2A/B were significantly reduced in knockout and G544D neurons by ~60% relative to the WT (Fig. 4E). Furthermore, when we analysed the co-localization of Doc2A/B with SV2 using Pearson's coefficient, we found a significant ~25% reduction in knockout and G544D neurons relative to the WT (Fig. 4F). In summary, we found that Doc2A/B forms aggregates in the presence of Munc18-1 missense mutants and trafficking of Doc2A/B to the synapse is impaired by depletion of functional Munc18-1.

Haploinsufficiency and disease-linked heterozygous Munc18-1 mutations reduce Doc2A/B levels and solubility

Our data have demonstrated that loss of Munc18-1 results in changes in Doc2 levels, solubility and localization. Yet, Munc18-1 patients typically carry one mutant and one WT allele of Munc18-1. To determine how Munc18-1 effectors are impacted in the disease-relevant heterozygous context, we generated constitutive Munc18-1 heterozygous knockout mice by crossing double-floxed Munc18-1 mice[56] with mice expressing Cre under the constitutive β-actin promoter.[58] Munc18-1 heterozygous knockout mice were born according to Mendelian ratio and revealed no morbidity (data not shown). When we analysed brains of heterozygous knockout mice at 3 months of age, we found them to express ~50% Munc18-1, confirming the successful removal of one allele (Fig. 5A). We also found a ~40% reduction in Doc2A/B levels

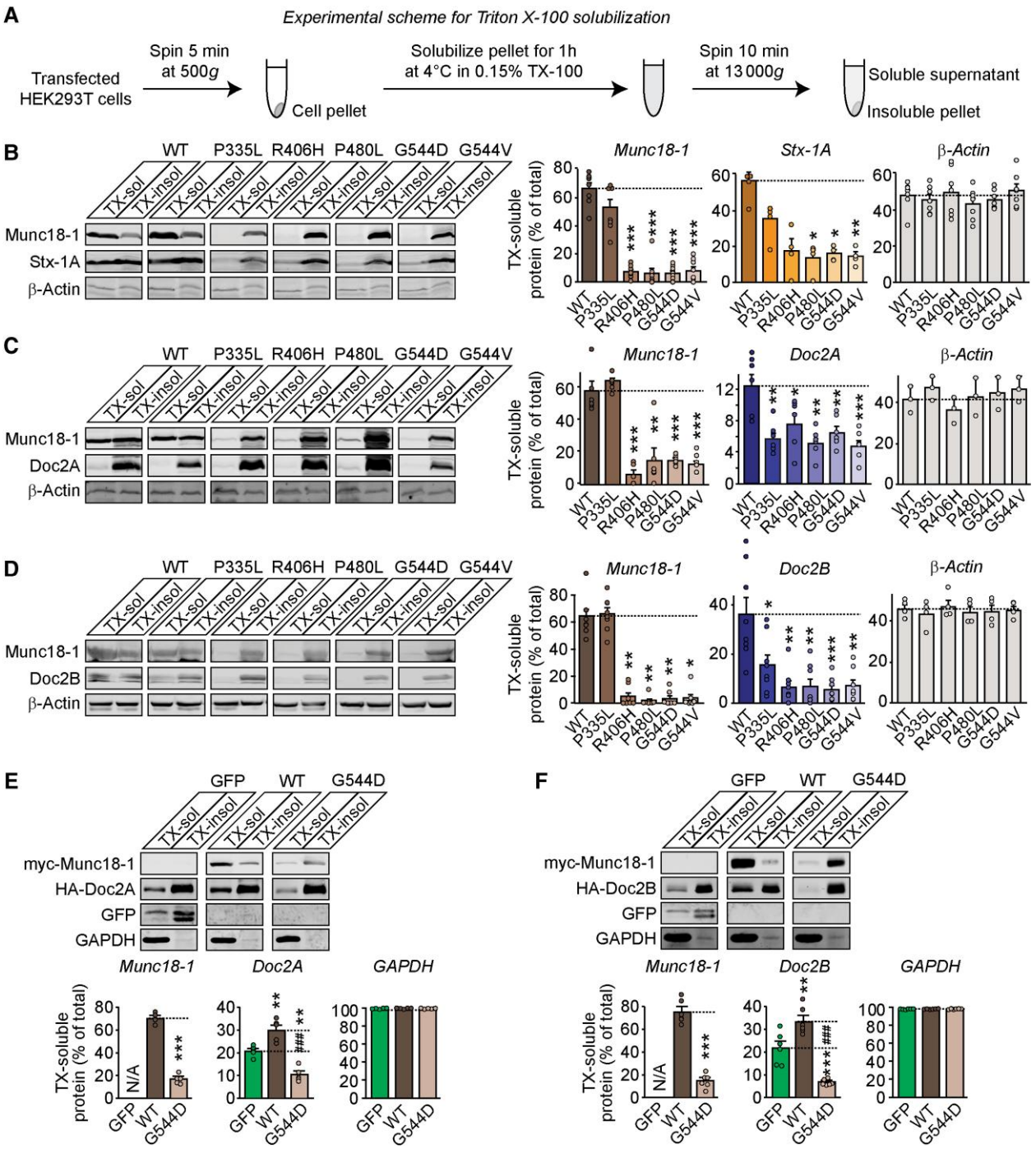

Figure 2 Reduced solubility of syntaxin-1, Doc2A and Doc2B in the presence of mutant Munc18-1. (**A**) Experimental scheme of the detergent solubility assay. (**B–D**) Solubility of syntaxin-1, Doc2A and Doc2B. Wild-type (WT) and five missense mutants of Munc18-1 were co-expressed with syntaxin-1A (**B**), HA-tagged Doc2A (**C**) or HA-tagged Doc2B (**D**) in HEK293T cells. Two days after transfection, cells were solubilized in 0.1% Triton X-100 (TX). Equal volumes of TX-soluble (TX-sol) and -insoluble (TX-insol) fractions were separated by SDS-PAGE, and TX-soluble protein was measured as the percentage of total protein by quantitative immunoblotting. (**E** and **F**) The absence of WT Munc18-1 and presence of G544D Munc18-1 differentially affected Doc2 solubility. Doc2A (**E**) or Doc2B (**F**) were expressed alone (GFP) or co-expressed with WT or G544D Munc18-1. The Triton X-100 solubility assay was performed and analysed as described earlier. One-way ANOVA with Tukey–Kramer *post hoc* test or Kruskal–Wallis test with Dunn's *post hoc* test; $^{*}P < 0.05$, $^{**,\#\#}P < 0.01$, $^{***}P < 0.001$; $n = 4$–8 independent experiments. Data are presented as mean ± standard error of the mean. SDS-PAGE = sodium dodecyl-sulphate polyacrylamide gel electrophoresis; Stx-1A = syntaxin-1A.

(Fig. 5A), in contrast to the unchanged levels previously observed in E18 Munc18-1 heterozygous knockout mouse brains.[56]

Are heterozygous missense mutations in Munc18-1 sufficient to rescue Doc2A/B levels, and/or do they exert a gain-of-function effect? Due to the lack of an available mouse model expressing a Munc18-1 missense mutant, we cultured cortical neurons from Munc18-1 floxed/WT mice lentivirally expressing ΔCre, Cre or Cre + G544D. Expression of Cre reduced total Munc18-1 levels by

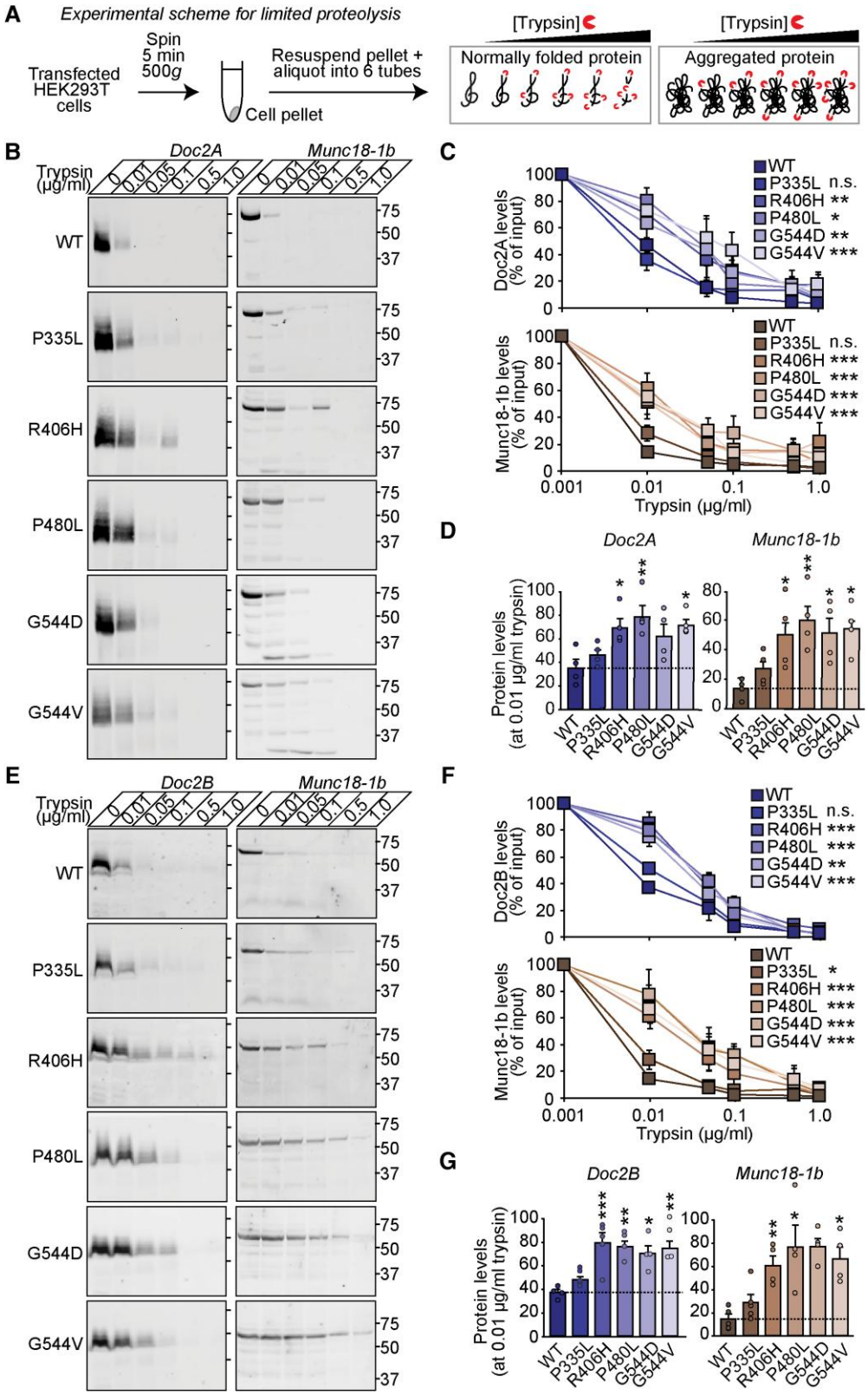

Figure 3 Doc2a and Doc2B aggregate in the presence of mutant Munc18-1. (**A**) Experimental scheme of the limited proteolysis assay. (**B–G**) Wild-type (WT) or mutant Munc18-1 were co-expressed with Doc2A (**B–D**) or Doc2B (**E–G**) in HEK293T cells. Two days after transfection, cell homogenates were subjected to limited proteolysis using the indicated concentrations of trypsin. The remaining protein levels were quantified by immunoblotting to the indicated protein. Two-way ANOVA (**C** and **F**) or one-way ANOVA with Tukey–Kramer *post hoc* test or Kruskal–Wallis test with Dunn's *post hoc* test (**D** and **G**); $^{*}P < 0.05$, $^{**}P < 0.01$, $^{***}P < 0.001$; $n = 4–6$ independent experiments. Data are presented as mean ± standard error of the mean. n.s. = not significant.

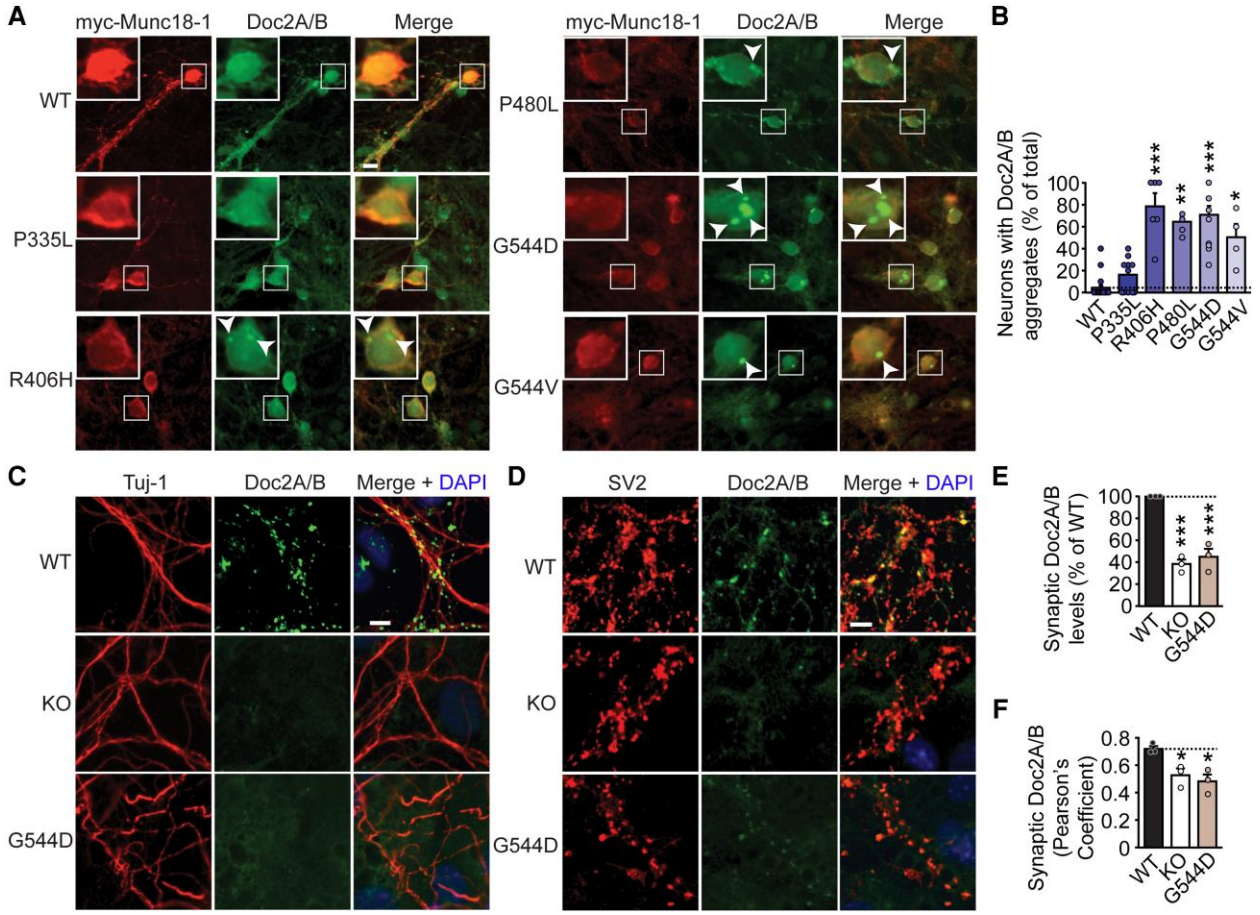

Figure 4 Aggregation and mislocalization of Doc2A/B in the presence of mutant Munc18-1. (**A** and **B**) Double-floxed Munc18-1 neurons were transduced with lentiviral vectors expressing Cre recombinase alone (KO) or along with either wild-type (WT) or mutant Munc18-1 at 6 days *in vitro* (DIV6). The subcellular localization of Munc18-1 and Doc2A/B was analysed by immunocytochemistry on DIV20. Arrows depict Doc2A/B aggregates (**A**) whose numbers were quantified (**B**). One-way ANOVA with the Tukey–Kramer *post hoc* test or Kruskal–Wallis test with Dunn's *post hoc* test; $^{*}P < 0.05$, $^{**}P < 0.01$, $^{***}P < 0.001$; $n = 4$–21 fields, 1–25 neurons per field. (**C**–**F**) Double-floxed Munc18-1 neurons were transduced with lentiviral vectors expressing Cre recombinase alone (KO) or along with WT or G544D Munc18-1 at DIV6. At DIV20, neurons were analysed for the localization of Doc2A/B relative to Tuj-1 (**C**) and SV2 (**D**–**F**) by immunocytochemistry. Doc2A/B immunofluorescence was quantified under an SV2 mask (**E**), and co-localization of Doc2A/B with SV2 was quantified using Pearson's coefficient (**F**). One-way ANOVA with Tukey–Kramer *post hoc* test; $^{*}P < 0.05$, $^{***}P < 0.001$; $n = 3$ independent experiments. Data are presented as mean ± standard error of the mean. Scale bars in **A**, **C** and **D** = 10 µm.

~50%, similar to our heterozygous knockout mice, and expression of G544D reduced total Munc18-1 levels by ~70%, a significant decrease from both WT and heterozygous knockout levels (Fig. 5B). When we quantified the levels of Doc2A/B, we found a ~40% reduction in heterozygous knockout neurons and ~60% reduction in heterozygous knockout neurons expressing G544D (Fig. 5B), suggesting that aggregation-prone G544D has an additional effect on Doc2A/B that results in significantly reduced Doc2A/B levels compared with heterozygous knockout neurons.

To determine whether the reduced Munc18-1 levels and/or presence of Munc18-1 missense mutations in the disease-like heterozygous knockout or heterozygous G544D contexts cause Doc2A/B to aggregate, we repeated the Triton X-100 solubility assay in cortical neurons cultured as in Fig. 5B. We observed that the solubility of Munc18-1 in the heterozygous knockout neurons was unchanged from WT, but in the heterozygous G544D neurons, Munc18-1 solubility was reduced by ~15% (Fig. 5C), as expected from our previous results.[18] Interestingly, we observed that endogenous Doc2A/B is highly insoluble (~100%) in our cortical neurons and that this insolubility is not altered in Munc18-1 heterozygous knockout or heterozygous G544D neurons (Fig. 5C). Other neuronal proteins revealed no change in solubility (Supplementary Fig. 9A). Note that the baseline solubility of all proteins differs due to their different biochemical properties. In transfected HEK293T cells, we observed that the solubility of Doc2A and Doc2B was also very low (Fig. 2C–F), indicating that the high Triton X-100 insolubility of Doc2A/B is not an artifact of exogenous overexpression in heterologous cells but indeed a normal feature of endogenous neuronal Doc2A/B as well. In addition to aggregates, Triton X-100 does not solubilize cholesterol-rich membranes, raising the possibility that endogenous Doc2A/B is predominantly bound to cholesterol-rich membranes, requiring alternative methods to assess Doc2A/B solubility in neurons.

Consequently, we again used limited proteolysis to assess the solubility of Doc2A/B under native conditions, in the absence of detergent. We found that, while the susceptibility of Munc18-1 to tryptic degradation was not significantly altered between WT and heterozygous knockout neurons, Munc18-1 was significantly more resistant to tryptic degradation in the heterozygous G544D neurons (Fig. 5D). When we measured the susceptibility of Doc2A/B to tryptic degradation, we found that Doc2A/B was more

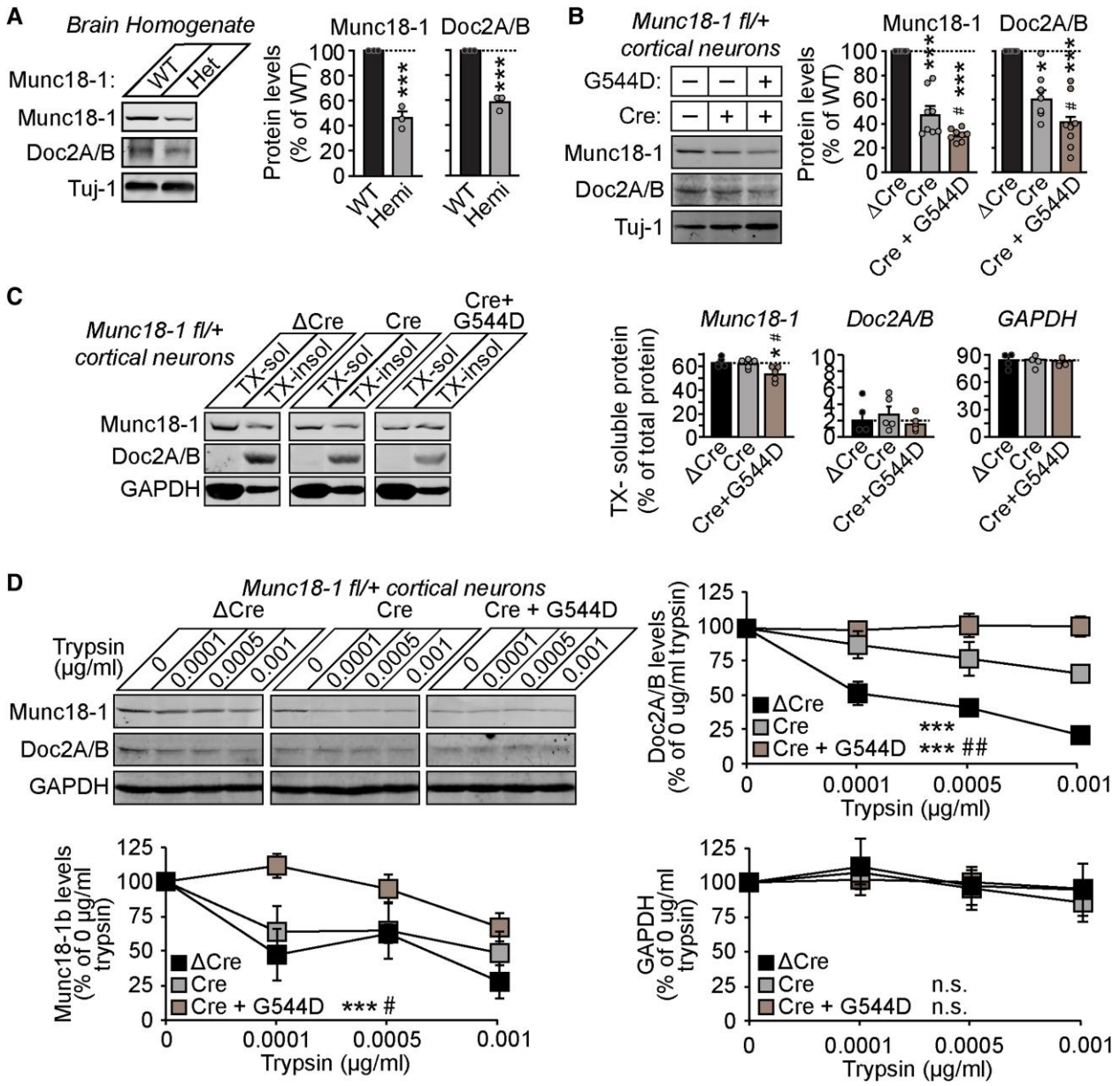

Figure 5 Disease-linked heterozygous Munc18-1 mutants reduce Doc2A/B levels. (**A**) Brains from 3-month-old littermate wild-type (WT) and heterozygous knockout Munc18-1 mice were homogenized and Doc2A/B protein levels in Munc18-1 heterozygous knockout mouse brains were quantified by immunoblotting, normalized to Tuj1 levels. Student's *t*-test; $^{***}P < 0.001$; $n = 3$ mice each. (**B**) Analysis of Doc2A/B protein levels in Munc18-1 heterozygous knockout neurons with or without lentiviral expression of Munc18-1 G544D. Neurons were transduced with lentiviral vectors expressing Cre recombinase (Cre), Cre recombinase plus G544D (Cre + G544D) or inactive Cre (ΔCre) at 6 days *in vitro* (DIV6). Levels of indicated proteins were analysed at DIV20 by quantitative immunoblotting, normalized to Tuj1 levels. One-way ANOVA with Tukey–Kramer *post hoc* test; $^{*,\#}P < 0.05$, $^{***}P < 0.001$; $n = 8$ independent experiments. (**C**) Analysis of Doc2A/B solubility in Munc18-1 heterozygous knockout neurons with or without lentiviral expression of Munc18-1 G544D. Neurons were transduced with lentiviral vectors expressing Cre, (Cre + G544D) or ΔCre at DIV6 and solubilized in 0.1% Triton X-100 (TX) on DIV20. Equal volumes of TX-soluble and -insoluble fractions were separated by SDS-PAGE, and TX-soluble protein was measured as the percentage of total protein by quantitative immunoblotting. One-way ANOVA with Tukey–Kramer *post hoc* test; $^{*,\#}P < 0.05$; $n = 5$ independent experiments. (**D**) Analysis of Doc2A/B aggregation in Munc18-1 heterozygous knockout neurons with or without lentiviral expression of Munc18-1 G544D. Neurons were transduced with lentiviral vectors expressing Cre, Cre + G544D or ΔCre at DIV6 and subjected to limited proteolysis using the indicated concentrations of trypsin. The remaining protein levels were quantified by immunoblotting to the indicated protein. Two-way ANOVA; $^{*,\#}P < 0.05$, $^{\#\#}P < 0.01$, $^{***}P < 0.001$; $n = 4$–5 independent experiments. Data are presented as mean ± standard error of the mean. SDS-PAGE = sodium dodecylsulphate polyacrylamide gel electrophoresis.

resistant to tryptic degradation in the heterozygous knockout neurons than the WT neurons (Fig. 5D), indicating that the reduction in Munc18-1 levels resulted in insolubility of Doc2A/B. Furthermore, we found that Doc2A/B was significantly more resistant to tryptic degradation in the heterozygous G544D neurons than in both the WT and heterozygous knockout neurons (Fig. 5D), indicating that the presence of a misfolding missense mutant such as G544D can exacerbate the insolubility of Doc2A/B observed in the haploinsufficiency-mimicking heterozygous knockout context.

However, since the total levels and solubility of Munc18-1 in the heterozygous G544D neurons are lower than in the heterozygous knockout neurons, it is unclear whether the additional effect of G544D on the total levels and insolubility of Doc2A/B is due to the further reduction of total and soluble Munc18-1 available to chaperone Doc2A/B or to the presence of the mutant Munc18-1 itself exerting a direct destabilizing effect. To better understand whether WT and G544D Munc18-1 expressed at similar levels have different impacts on Doc2A/B levels, we cultured cortical neurons from P0 Munc18-1 conditional knockout mice and lentivirally expressed Cre and WT (1×) or G544D (1×) Munc18-1 as before. Additionally, we lentivirally expressed Cre and added amounts of WT lentivirus (0.01× and 0.05×) expected to match the total protein levels previously observed for G544D Munc18-1 at ∼1%–5% of WT.[18] We found that 0.01× WT, 0.05× WT and 1× G544D resulted in similar levels of Munc18-1 at ∼2%–6% compared with 1× WT (although only 1× G544D resulted in reduced Munc18-1 solubility in Triton X-100 solubility compared with 1× WT) and in similar levels of Doc2A/B at ∼20%–40% (Supplementary Fig. 9B–D). This suggested that Doc2A/B levels depend more on the overall level of Munc18-1 expression and less on the particular variant expressed.

To determine whether titrating in additional WT Munc18-1 can overcome the effect of G544D Munc18-1 on Doc2A/B, we again cultured cortical neurons from P0 Munc18-1 conditional knockout mice and lentivirally expressed Cre and WT Munc18-1 (100% WT), G544D Munc18-1 with no WT Munc18-1 (G544D + 0% WT) or G544D Munc18-1 with increasing amounts of WT Munc18-1 lentivirus (G544D + 1%, 5%, 10% or 50% WT). We found that in G544D + 0% WT neurons, Munc18-1 levels were reduced to ∼10% compared with 100% WT, and, interestingly, none of the amounts of WT lentivirus added to G544D-expressing neurons was able to rescue Munc18-1 levels to greater than ∼20% relative to the 100% WT neurons (Supplementary Fig. 9E and F). As expected, the Triton X-100 solubility of Munc18-1 was also reduced in the G544D + 0% WT neurons and could not be rescued by any of the amounts of WT lentivirus that we added (Supplementary Fig. 9E and H). These data suggested that the presence of G544D Munc18-1 suppresses WT Munc18-1 levels and solubility. However, the G544D + 50% WT neurons did achieve a significant increase in Munc18-1 levels compared with G544D + 0% WT neurons (Supplementary Fig. 9E and G), indicating that even greater expression of WT Munc18-1 may be able to overcome that suppression. Furthermore, Doc2A/B levels were reduced to ∼40% in G544D + 0% WT neurons relative to 100% WT neurons, and although Doc2A/B trended toward an increase with the addition of WT Munc18-1, none of the amounts of WT lentivirus added to G544D-expressing neurons was able to fully rescue Doc2A/B levels relative to 100% WT neurons or achieve a statistically significant increase of Doc2A/B levels relative to G544D + 0% WT neurons (Supplementary Fig. 9E–G).

Munc18-1 mutations impair the synaptic localization of Doc2A/B

We next analysed whether disease-causing mutations in Munc18-1 impair synaptic localization of Doc2A/B. We cultured cortical Munc18-1$^{fl/+}$ neurons expressing ΔCre, Cre or Cre+G544D Munc18-1 and immunostained them for both Doc2A/B and the presynaptic protein SV2 (Fig. 6A). We first quantified Doc2A/B immunofluorescence under an SV2 mask and found a ∼30% reduction in synaptic Doc2A/B levels in the Munc18-1$^{fl/+}$ neurons expressing Cre and a ∼50% reduction in the Munc18-1$^{fl/+}$ neurons expressing Cre and G544D Munc18-1, which were both significantly different from WT and from each other (Fig. 6B). Next, we measured co-localization of Doc2A/B with SV2 using Pearson's coefficient, which only measures patterns and not intensity levels, and found that co-localization was reduced by ∼25% in Munc18-1$^{fl/+}$ neurons expressing Cre both with and without G544D Munc18-1, relative to WT (Fig. 6C). These data indicated that cultured cortical Munc18-1$^{fl/+}$ neurons expressing Cre with and without G544D Munc18-1 not only have reduced synaptic levels of Doc2A/B but also reduced synaptic targeting of Doc2A/B that cannot be explained by the decreased Doc2A/B levels alone. The data also revealed that the additional effect we observed on Doc2A/B levels in Munc18-1$^{fl/+}$ neurons expressing Cre + G544D Munc18-1 relative to Munc18-1$^{fl/+}$ neurons expressing Cre alone does not exacerbate this synaptic targeting impairment, suggesting that the reduction of Munc18-1 levels to ∼50% is sufficient to trigger this deficit.

To determine how the reduction of Doc2A/B total levels and the impairment of Doc2A/B synaptic targeting combine to impact the amount of physiologically relevant Doc2A/B available at the synapse, we homogenized Munc18-1 WT and heterozygous knockout mouse brains and enriched for synaptosomes using subcellular fractionation (Fig. 6D and E). We found that the ratio of synaptosomal to total protein was unchanged for Munc18-1 in heterozygous knockout mice (Fig. 6F) but reduced to ∼45% for Doc2A/B (Fig. 6G). We also enriched for synaptosomes from cultured cortical Munc18-1 WT (ΔCre), heterozygous knockout (Cre) and heterozygous knockout expressing G544D (Cre + G544D) neurons (Fig. 6D and H), and found, similar to what we observed in heterozygous knockout mouse brains, that the ratio of synaptosomal to total protein was not significantly altered in the heterozygous knockout or heterozygous knockout expressing G544D contexts for Munc18-1 (Fig. 6I), but was reduced for Doc2A/B in both genotypes to ∼25–30% of WT neurons (Fig. 6J).

Doc2A/B partially rescues impairments in synaptic function caused by Munc18-1 haploinsufficiency

To determine whether the reduced levels, reduced solubility and impaired localization of Doc2A/B observed in our heterozygous knockout and heterozygous G544D cortical neurons contribute to synaptic deficits, we measured spontaneous individual neuronal activity as well as network activity using a multi-electrode array (Fig. 7A–E) in cultured cortical neurons from P0 WT and Munc18-1 heterozygous knockout mice, in addition to lentivirally expressed G544D Munc18-1 in half of the wells of each Munc18-1 heterozygous knockout plate. We found that, whereas the mean firing rate of heterozygous knockout neurons was unchanged relative to the WT, the mean firing rate of heterozygous knockout + G544D neurons was significantly reduced by ∼37% and ∼40% relative to the WT and heterozygous knockout neurons, respectively (Fig. 7B). Interestingly, lentiviral expression of Doc2A and Doc2B rescued the mean firing rate in heterozygous knockout + G544D neurons and did not affect the mean firing rate of heterozygous knockout neurons. We also found that compared to heterozygous knockout neurons, heterozygous knockout + G544D neurons exhibited a significant reduction in inter-burst interval that could be rescued by lentiviral expression of Doc2A and Doc2B (Fig. 7C).

We next measured spontaneous network activity and found that heterozygous knockout neurons and heterozygous knockout + G544D neurons showed a significantly reduced network burst frequency (by 55% and ∼70%, respectively) and duration (by 26% and

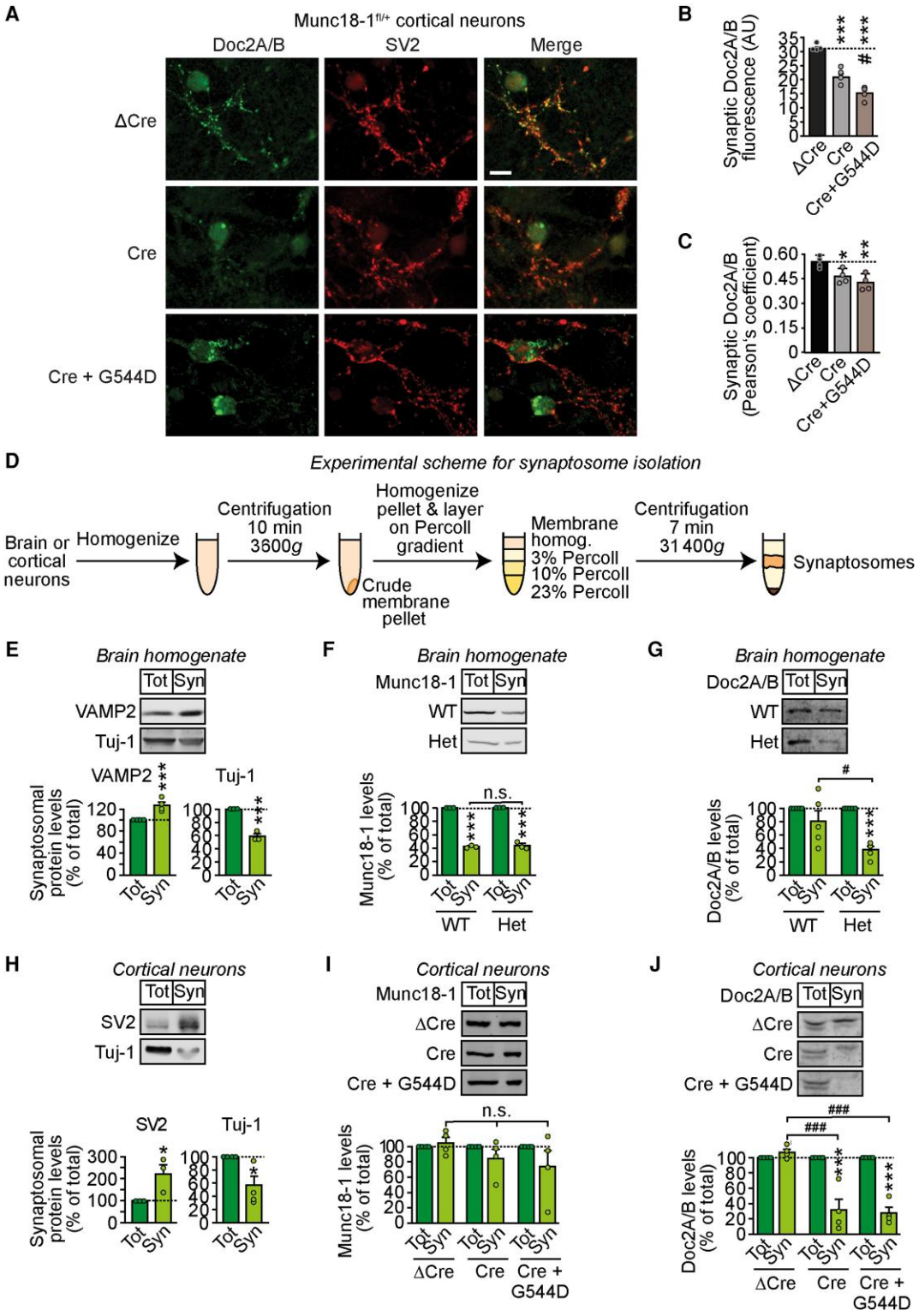

Figure 6 Disease-linked heterozygous Munc18-1 mutants reduce the synaptic localization of Doc2A/B. (**A–C**) Synaptic localization of Doc2A/B. Neurons were transduced with lentiviral vectors expressing Cre recombinase (Cre), Cre recombinase plus G544D (Cre + G544D) or inactive Cre (ΔCre) at 6 days *in vitro* (DIV6) and analysed for the localization of Doc2A/B relative to SV2 by immunocytochemistry (**A**). Scale bar = 10 µm. Doc2A/B immunofluorescence was quantified under an SV2 mask (**B**) or co-localization of Doc2A/B with SV2 was quantified using Pearson's coefficient (**C**). One-way ANOVA with Tukey–Kramer *post hoc* test; $^{*,\#}P < 0.05$, $^{***}P < 0.001$; $n = 3$. (**D**) Experimental scheme for the synaptosome isolation experiment. (**E–G**) Enrichment analysis of proteins in synaptosomal preparations from brain. Brains of 3-month-old Munc18-1 wild-type (WT) or heterozygous knockout mice were homogenized and subjected to subcellular fractionation to yield synaptosomes. Twenty micrograms of brain homogenate and synaptosomes were analysed by quantitative immunoblotting of the indicated proteins. One-way ANOVA with Tukey–Kramer *post hoc* test; $^{***}P < 0.001$, $^{\#}P < 0.05$; $n = 3$–5 mice each. **H–J** are the same as in **E–G**, except that synaptosomal preparations were done from cultured WT (ΔCre), heterozygous (Cre) or heterozygous G544D-expressing Munc18-1 neurons (Cre + G544D). One-way ANOVA with Tukey–Kramer *post hoc* test; $^{*}P < 0.05$, $^{***}P < 0.001$, $^{\#\#\#}P < 0.001$; $n = 3$–4 independent experiments. All data are presented as mean ± standard error of the mean.

32%, respectively) (Fig. 7D and E). Lentiviral expression of Doc2A and Doc2B in heterozygous knockout neurons resulted in an intermediate network burst frequency that was not statistically significantly different from either the WT or heterozygous knockout phenotype but did not rescue the network burst frequency of heterozygous knockout + G544D neurons or the network burst duration phenotype for either heterozygous knockout neurons or heterozygous knockout + G544D neurons (Fig. 7D and E).

We next measured synaptic vesicle cycling using the uptake of an antibody that recognizes a luminal epitope of the synaptic vesicle protein synaptotagmin-1 that is exposed to the extracellular media when synaptic vesicles fuse with the plasma membrane and then internalized along with the bound antibody when synaptotagmin-1 is endocytosed. Our intention was not to demonstrate a specific effect on a specific step in neurotransmitter release but rather general deficits in synaptic vesicle cycling using this well-established technique, particularly because of the multitudinous and unclear proposed effects of Doc2 on neurotransmitter release.[45,48-51,66,69-74] We cultured cortical neurons from P0 WT and Munc18-1 heterozygous knockout mice, and additionally lentivirally expressed G544D Munc18-1 in half of the wells of each Munc18-1 heterozygous knockout plate. We then stimulated these neurons expressing WT or mutant Munc18-1 with high potassium and quantified the fluorescence intensity of endocytosed anti-synaptotagmin-1 antibody at synapses (using a synaptic mask created from SV2 immunofluorescence). We found that synaptotagmin-1 uptake was reduced by ~33% in heterozygous knockout neurons and by ~47% in heterozygous knockout + G544D neurons (Fig. 7F and G). When we lentivirally expressed Doc2A and Doc2B in heterozygous knockout neurons and heterozygous knockout neurons expressing G544D, we observed partial rescues of anti-synaptotagmin-1 uptake to 83% and 79% of WT, respectively.

In addition to the antibody uptake assay, we measured the exocytosis-dependent change in fluorescence emitted by the synaptic vesicle-localized chimeric protein synaptophysin pHluorin.[75] pHluorin is quenched in the acidic synaptic vesicle lumen, but upon the fusion of synaptic vesicles to the presynaptic plasma membrane, it is exposed to the relatively neutral extracellular pH[76,77] and emits light. When we treated WT neurons with elevated extracellular potassium (55 mM) for 1 min, we observed a change in fluorescence over baseline ($\Delta F/F_i$) representing ~22% of the total vesicle pool (revealed by treating neurons with 50 mM NH_4Cl) compared with ~11% in heterozygous knockout neurons and only ~6% in heterozygous knockout + G544D neurons (Fig. 7H and I). When we lentivirally expressed Doc2A and Doc2B in heterozygous knockout neurons and heterozygous knockout + G544D neurons, we observed partial rescues from 11% to ~16% and from 6% to ~12%, respectively (Fig. 7H and I).

The mixture of rescue efficiencies observed in the multi-electrode array, antibody uptake and pHluorin assays suggest that, while lentiviral Doc2A/B expression can restore some synaptic function in mutant neurons, other proteins that support synaptic function are likely to be impaired as well.

Discussion

The molecular mechanisms underlying STXBP1 encephalopathies are only poorly understood. Reductions in Munc18-1 levels and/or a gain-of-toxic function of Munc18-1 missense mutants have been described.[5,17,18,57,64] However, it remains unclear if other proteins, in particular proteins that interact with Munc18-1, are affected. Here, we found that reduced levels of Munc18-1 also lead to a reduction in the levels of some of its well-established interactors, including syntaxin-1 and Doc2A/B, and that Munc18-1 missense mutants can exacerbate that reduction. Our data suggest that STXBP1 encephalopathies are not only characterized by dysfunctional Munc18-1 but also by dysfunction of the Munc18-1 binding partners syntaxin-1 and Doc2A/B, and potentially other proteins. We propose a model in which Munc18-1 stabilizes Doc2A and Doc2B levels and facilitates their localization to the synapse (Fig. 8). The reduction in Munc18-1 levels caused by mutations in Munc18-1 in STXBP1 encephalopathies causes a reduction in Doc2A/B levels and impairs the ability of remaining Doc2A/B to localize to the synapse, contributing to synaptic dysfunction (Fig. 8). Our data further suggest that some Munc18-1 missense mutations trigger co-aggregation and further destabilization of Doc2A/B, which may at least partially explain the heterogeneity of symptoms across patients with different mutations (Fig. 8).

Phenotypes are rarely consistent across genetic backgrounds and, in extreme cases, result in distinct conditions even with the same causal DNA sequence in individuals. These genetic background effects often result from the action of modifier genes, through either direct interaction with the target gene product, mechanistic contribution to the same biological process and/or functional compensation through alternative pathways (reviewed by Riordan and Nadeau[78]). Interestingly, thousands of single nucleotide polymorphisms (SNPs) have been reported for both DOC2A and DOC2B, including 3′ UTR variants, 5′ UTR variants, intron variants, missense variants, splice site variants and nonsense variants.[79-82] Some of these variants are linked to traits such as body mass index, height, Alzheimer's disease, executive function measurements, insomnia and sexual dimorphism.[80] For others, no data exist. Such SNPs in DOC2A and DOC2B may modify the phenotypic outcome of the primary disease-causing mutations in STXBP1 and thereby affect the severity of the disease condition via enhancing or suppressing phenotypes to varied degrees, depending on the SNP, without being disease-causing themselves. To our knowledge, no modifier gene study for STXBP1 encephalopathies exists so far but would be extremely valuable, particularly in individuals who share the same genetic mutation in STXBP1.

The extent to which the reduction in functional Doc2A/B levels contributes to STXBP1-E disease phenotypes is not known. Doc2A and Doc2B are differentially expressed in glutamatergic and GABAergic neurons, respectively,[68] as well as in complementary brain regions.[27] This suggests that a potential impact of mutant Munc18-1 on one or both Doc2 proteins could have different effects depending on the cell types and areas of the brain in which they are expressed (Fig. 8). For example, since Doc2B is only or predominantly expressed in GABAergic neurons, an impairment of Doc2B-mediated synaptic functions by mutant Munc18-1 could result in an imbalance between excitation and inhibition that in turn may cause seizures and/or disrupt network properties required for normal brain function. For example, in Doc2B knockout brains, spontaneous inhibitory postsynaptic current frequency was reduced by approximately 75% in Purkinje cells, and the resulting disinhibition caused a continuous and unrelenting spiking pattern that was not observed in WT recordings.[45] Additionally, there appear to be cell-type specific consequences in Munc18-1 heterozygous knockout mouse brains, with a greater impairment of inhibitory neurons than excitatory neurons.[83]

Most studies agree that depleting Doc2A and Doc2B results in a reduction of spontaneous release from excitatory and inhibitory synapses, respectively.[45,48,68,84] Interestingly, one group found

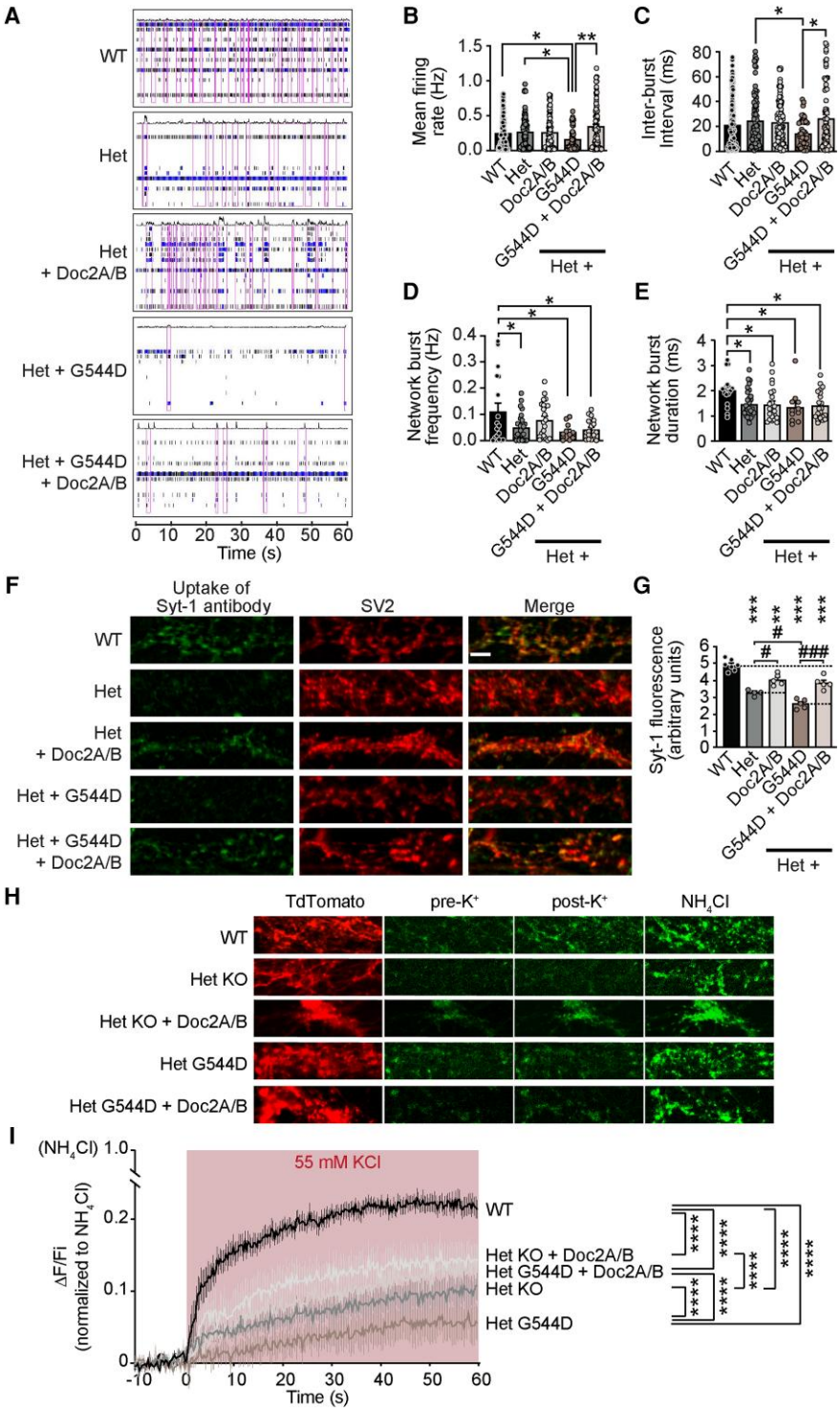

Figure 7 Synaptic impairments in haploinsufficient and heterozygous G544D neurons and differential partial rescue with Doc2A/B. (**A**–**E**) Analysis of spontaneous neuronal activity. Munc18-1 wild-type (WT), heterozygous knockout (with and without overexpression of Doc2A/B) and heterozygous knockout + G544D (with and without overexpression of Doc2A/B) were cultured on a multi-electrode array with 16 electrodes per well (**A**) and analysed at 14 days *in vitro* (DIV14) for mean firing rate (**A** and **B**), inter-burst interval (**A** and **C**), network burst frequency (**A** and **D**) and network burst duration (**A** and **E**). Purple boxes in **A** indicate network burst activity. One-way ANOVA with Šídák's *post hoc* test or Kruskal–Wallis with Dunn's *post hoc* test; $^{*}P < 0.05$, $^{**}P < 0.01$; $n = 70$–244 independent experiments. (**F** and **G**) Neurons cultured as above were stimulated by high potassium and subjected to an antibody uptake assay. Endocytosed anti-synaptotagmin-1 (Syt-1) antibody was quantified by measuring immunostaining under a synaptic mask derived from the SV2 signal. One-way ANOVA with Šídák's *post hoc* test; $^{\#}P < 0.05$, $^{**}P < 0.01$, $^{***,\#\#\#}P < 0.001$; $n = 4$–7 independent experiments. Scale bar = 5 µm. (**H** and **I**) Munc18-1 WT, heterozygous knockout (with and without overexpression of Doc2A/B), and heterozygous knockout + G544D (with and without overexpression of Doc2A/B) neurons lentivirally expressing synaptophysin-pHluorin (SypHy) were stimulated by treatment with 55 mM potassium chloride (KCl) and the change in SypHy fluorescence over baseline ($\Delta F/F_i$) normalized to the total vesicle pool (revealed by treatment with NH_4Cl) was analysed. Two-way ANOVA with Bonferroni's *post hoc* test; $^{****}P < 0.0001$; $n = 6$–11 independent experiments. All data are presented as mean ± standard error of the mean.

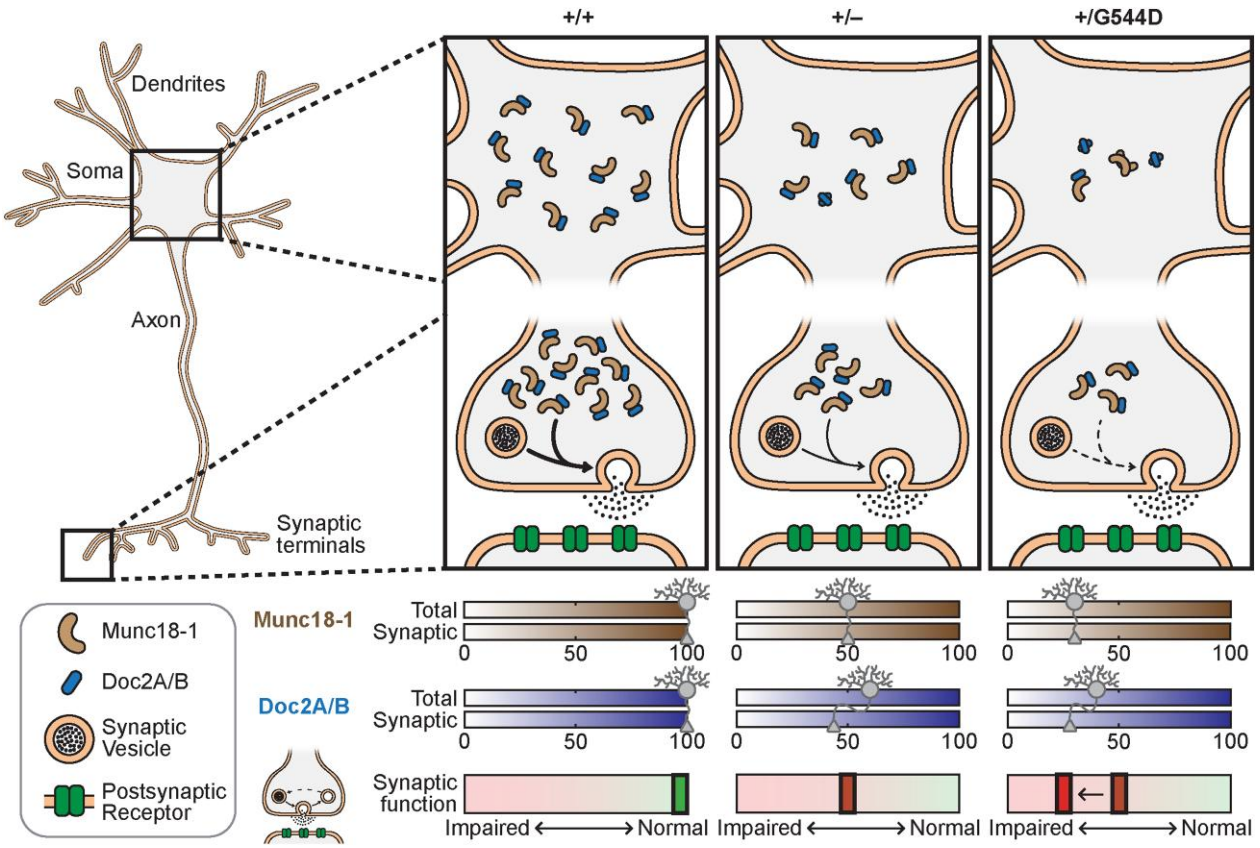

Figure 8 Proposed model of Doc2A/B dysfunction in STXBP1 encephalopathies. Munc18-1 and Doc2A/B are present in both the soma and the synaptic terminals, where they execute their function in neurotransmitter release. In wild-type (WT) neurons, normal levels, intact subcellular localization and lack of aggregation facilitate proper neurotransmitter release. With the loss of one copy of Munc18-1, both total and synaptic levels of Munc18-1 are reduced to 50%. Total Doc2A/B levels are reduced to 60%, while synaptic levels are depleted to below 50%, together resulting in impaired synaptic function. In heterozygous neurons expressing mutant G544D Munc18-1, total Munc18-1 levels are reduced to 30%, Doc2A/B levels are reduced to 40% and synaptic levels are even further reduced, together resulting in further impairment of synaptic function.

that rescuing with Doc2A but not Doc2B restored the miniature excitatory postsynaptic current deficit, and rescuing with Doc2B but not Doc2A restored the miniature inhibitory postsynaptic current deficit,[48] whereas another group found that expression of either Doc2A or Doc2B was sufficient to rescue the spontaneous release deficits observed in both the Doc2A and Doc2B knockouts, suggesting that although Doc2A and Doc2B are expressed in different cell types, they are functionally redundant.[68]

While some studies found that depletion of Doc2A/B did not affect evoked release,[45,48] other studies have found impairments in the asynchronous phase of evoked release,[49,51,72,73] a form of neurotransmitter release which becomes more and more dominant over synchronous release as rates of stimulation increase.[85] Furthermore, synaptic augmentation at 10 Hz (a form of short-term plasticity) is impaired in Doc2A/B double knockout neurons,[51] and hippocampal slices from Doc2A knockout mice exhibit significantly reduced long-term potentiation following 100 Hz tetanus.[50] Additionally, facilitation during 5 Hz stimulation declines more rapidly in Doc2A knockout compared with the WT but is unaffected at 1 Hz,[50] suggesting that Doc2 is required to sustain release under increasing rates of stimulation. Interestingly, Munc18-1 heterozygous knockout autaptic neurons have also been shown to have a reduced capacity to fully sustain release during intense stimulation relative to the WT,[69] a deficit in presynaptic function cited as a potential cause for the impairment in long-term potentiation also observed in heterozygous Munc18-1 knockout hippocampal slices.[86] However, depleting Doc2A/B levels alone is different from changing its solubility and subcellular localization in the presence of mutant Munc18-1, as shown here, and therefore, different phenotypes may arise. While it is unknown how the global reduction of Munc18-1 levels results in differential impairments among different neuronal cell types, the impairment of Munc18-1 binding partners with their different expression patterns in the brain may point toward an explanation and needs to be further explored.

In addition to potential phenotypic differences caused by a reduction in different Doc2 isoforms, the disease phenotype is also affected by changes to different neuronal subtypes. The importance of GABAergic dysfunction in STXBP1 encephalopathies is highlighted by the observation that in Munc18-1 heterozygous knockout mice, which exhibit cortical hyperexcitability and seizures, parvalbumin-expressing and somatostatin-expressing interneurons are impaired in distinct ways, with parvalbumin-expressing interneurons exhibiting a reduction in synaptic strength and somatostatin-expressing interneurons exhibiting a decrease in connectivity.[83]

Our data revealed a ~40% reduction of Doc2A/B levels in Munc18-1 heterozygous knockout mouse brains and cultured cortical neurons, while in the presence of the missense mutation G544D, Doc2A/B were reduced by ~60%. Furthermore, in the heterozygous knockout mouse brains and heterozygous neurons with and without G544D Munc18-1 expression, the ratio of synaptosomal to

total Doc2A/B was reduced by ~60%–75% relative to the WT, indicating that in addition to the overall reduction of Doc2A/B levels, there was an impairment in Doc2A/B targeting of the synapse. The threshold at which Doc2A/B levels impair spontaneous glutamatergic and GABAergic release is currently unknown.

The effect of mutant Munc18-1 on functional Doc2A/B levels may in fact be even greater than the effect we observed on total Doc2A/B levels. For example, we found that Doc2A/B aggregate in the presence of mutant Munc18-1. It is possible that during the solubilization of cultured neurons in SDS-containing buffer, aggregated SDS-soluble Doc2A/B may have contributed to our quantification of total Doc2A/B. However, these aggregate species do not contribute to the pool of Doc2A/B available to subserve synaptic functions. In addition, the functional output of Doc2A/B may depend not only on its own abundance but also on the availability of its binding partner Munc18-1 and the influence of Munc18-1 on the levels and localization of other proteins such as syntaxin-1, which competes with Doc2A/B for Munc18-1 binding.[27] Furthermore, Doc2A/B levels reduced to a degree that may not ordinarily cause synaptic impairments could leave synapses with a diminished reserve pool of Doc2A/B that is insufficient for normal function under stressful conditions or as a consequence of ageing. Some indication of an age-dependent effect of Munc18-1 heterozygous knockout on its binding partners is given by the significant reduction of the levels of Doc2A/B in 3-month-old heterozygous knockout mouse brains (Fig. 5A), while a previous study found no change in those proteins in E18 heterozygous knockout embryos.[56] There is also clinical evidence for age-dependent effects in STXBP1 encephalopathies, with a subset of clinical features increasing in frequency with age, including intellectual disability, tremor, ataxia, generalized tonic-clonic seizures, absence seizures and EEGs with abnormally slow frequencies.[19]

However, we do not expect that dysfunction of Doc2A and Doc2B is the only source of pathology in STXBP1 encephalopathies. Indeed, overexpression of Doc2A and Doc2B only partially rescued the synaptic deficits we observed in heterozygous knockout neurons (Fig. 7). Munc18-1 interacts with and/or regulates the functions of numerous other synaptic proteins, including those with established relevance to disease such as syntaxin-1 and α-synuclein. Recently, a list of 176 potential downstream targets was published in induced neurons upon proteomic analysis.[74] However, none of the changes have yet been followed up and confirmed, and it currently remains unclear which of the changes are secondary, which tertiary, which are specific to the induced neuron model system and which are disease-relevant and/or compensatory. In addition, although we did not find that co-expression of the Munc18-1 interactors rab3, Mint1, and Mint2 with Munc18-1 missense mutations impaired their total levels or caused them to aggregate in heterologous cells, it may be that their physiological and/or pathological interactions require their endogenous neuronal context, and/or that Munc18-1 may disrupt the functions of different subsets of its interactors by distinct mechanisms, each contributing to the complex and variable phenotypes observed in patients.

Overall, our study demonstrates that STXBP1 encephalopathies are characterized not only by the reduction of functional Munc18-1 levels but also by a reduction in the functional levels of the Munc18-1 binding partners Doc2A and Doc2B. Further studies are required to determine how the overall reduction in Doc2A/B levels, coupled with the additional reduction in synaptic levels of Doc2A/B, contribute to what is observed clinically in STXBP1 encephalopathies.

Data availability

Raw data are available from the corresponding authors upon request.

Acknowledgement

We thank Dr Thomas C. Südhof for providing the Doc2A/B and SV2 antibody.

Funding

This work was supported by the American Epilepsy Society (924829 to A.B.), T32GM007739 (Weill Cornell/Rockefeller/Sloan Kettering Tri-Institutional MD PhD Program for D.A.), 1F30HD100096-01A1 (to D.A.), the Alzheimer's Association (NIRG-15-363678 to M.S.), American Federation for Aging Research (M.S.) and the National Institutes of Health (1R01-AG052505 and 1R01-NS095988 to M.S.; R01-NS102181, R01-NS113960, R21-NS127939 and R01-NS121077 to J.B.; 1RF1-NS126342-01 to M.S. and J.B.).

Competing interests

The authors report no competing interests.

Supplementary material

Supplementary material is available at *Brain* online.

References

1. Abramov D, Guiberson NGL, Burre J. STXBP1 encephalopathies: Clinical spectrum, disease mechanisms, and therapeutic strategies. *J Neurochem*. 2021;157:165-178.
2. Stamberger H, Nikanorova M, Willemsen MH, et al. STXBP1 encephalopathy: A neurodevelopmental disorder including epilepsy. *Neurology*. 2016;86:954-962.
3. Carvill GL, Weckhuysen S, McMahon JM, et al. GABRA1 and STXBP1: novel genetic causes of Dravet syndrome. *Neurology*. 2014;82:1245-1253.
4. Otsuka M, Oguni H, Liang JS, et al. STXBP1 mutations cause not only Ohtahara syndrome but also West syndrome–result of Japanese cohort study. *Epilepsia*. 2010;51:2449-2452.
5. Saitsu H, Kato M, Mizuguchi T, et al. De novo mutations in the gene encoding STXBP1 (MUNC18-1) cause early infantile epileptic encephalopathy. *Nat Genet*. 2008;40:782-788.
6. Hamdan FF, Piton A, Gauthier J, et al. De novo STXBP1 mutations in mental retardation and nonsyndromic epilepsy. *Ann Neurol*. 2009;65:748-753.
7. Hamdan FF, Gauthier J, Dobrzeniecka S, et al. Intellectual disability without epilepsy associated with STXBP1 disruption. *Eur J Hum Genet*. 2011;19:607-609.
8. Olson HE, Tambunan D, LaCoursiere C, et al. Mutations in epilepsy and intellectual disability genes in patients with features of Rett syndrome. *Am J Med Genet A*. 2015;167A:2017-2025.
9. Romaniello R, Saettini F, Panzeri E, Arrigoni F, Bassi MT, Borgatti R. A de-novo STXBP1 gene mutation in a patient showing the Rett syndrome phenotype. *Neuroreport*. 2015;26:254-257.
10. Dravet C, Oguni H. Dravet syndrome (severe myoclonic epilepsy in infancy). *Handb Clin Neurol*. 2013;111:627-633.
11. Hrachovy RA, Frost JD Jr. Infantile spasms. *Handb Clin Neurol*. 2013;111:611-618.

12. Yamatogi Y, Ohtahara S. Early-infantile epileptic encephalopathy with suppression-bursts, Ohtahara syndrome; its overview referring to our 16 cases. *Brain Dev*. 2002;24:13-23.
13. Ohtahara S, Yamatogi Y. Ohtahara syndrome: with special reference to its developmental aspects for differentiating from early myoclonic encephalopathy. *Epilepsy Res*. 2006;70(Suppl 1): S58-S67.
14. McTague A, Cross JH. Treatment of epileptic encephalopathies. *CNS Drugs*. 2013;27:175-184.
15. Panayiotopoulos CP, Benbadis SR, Covanis A, et al. Efficacy and tolerability of the new antiepileptic drugs I: Treatment of new onset epilepsy: Report of the therapeutics and technology assessment subcommittee and quality standards subcommittee of the American Academy of Neurology and the American Epilepsy Society. *Neurology*. 2005;64:172-174; author reply 172-4.
16. Saitsu H, Kato M, Okada I, et al. STXBP1 mutations in early infantile epileptic encephalopathy with suppression-burst pattern. *Epilepsia*. 2010;51:2397-2405.
17. Kovacevic J, Maroteaux G, Schut D, et al. Protein instability, haploinsufficiency, and cortical hyper-excitability underlie STXBP1 encephalopathy. *Brain*. 2018;141:1350-1374.
18. Guiberson NGL, Pineda A, Abramov D, et al. Mechanism-based rescue of Munc18-1 dysfunction in varied encephalopathies by chemical chaperones. *Nat Commun*. 2018;9:3986.
19. Xian J, Parthasarathy S, Ruggiero SM, et al. Assessing the landscape of STXBP1-related disorders in 534 individuals. *Brain*. 2022;145:1668-1683.
20. Aalto MK, Ruohonen L, Hosono K, Keranen S. Cloning and sequencing of the yeast Saccharomyces cerevisiae SEC1 gene localized on chromosome IV. *Yeast*. 1991;7:643-650.
21. Hosono R, Hekimi S, Kamiya Y, et al. The unc-18 gene encodes a novel protein affecting the kinetics of acetylcholine metabolism in the nematode Caenorhabditis elegans. *J Neurochem*. 1992;58: 1517-1525.
22. Grone BP, Marchese M, Hamling KR, et al. Epilepsy, behavioral abnormalities, and physiological comorbidities in syntaxin-binding protein 1 (STXBP1) mutant zebrafish. *PLoS One*. 2016; 11:e0151148.
23. Harrison SD, Broadie K, van de Goor J, Rubin GM. Mutations in the Drosophila Rop gene suggest a function in general secretion and synaptic transmission. *Neuron*. 1994;13:555-566.
24. Verhage M, Maia AS, Plomp JJ, et al. Synaptic assembly of the brain in the absence of neurotransmitter secretion. *Science*. 2000;287:864-869.
25. Pevsner J, Hsu SC. Scheller RH. n-Sec1: a neural-specific syntaxin-binding protein. *Proc Natl Acad Sci U S A*. 1994;91: 1445-1449.
26. Garcia EP, Gatti E, Butler M, Burton J, De Camilli P. A rat brain Sec1 homologue related to Rop and UNC18 interacts with syntaxin. *Proc Natl Acad Sci U S A*. 1994;91:2003-2007.
27. Verhage M, de Vries KJ, Roshol H, Burbach JP, Gispen WH, Sudhof TC. DOC2 proteins in rat brain: Complementary distribution and proposed function as vesicular adapter proteins in early stages of secretion. *Neuron*. 1997;18:453-461.
28. Graham ME, Handley MT, Barclay JW, et al. A gain-of-function mutant of Munc18-1 stimulates secretory granule recruitment and exocytosis and reveals a direct interaction of Munc18-1 with rab3. *Biochem J*. 2008;409:407-416.
29. Okamoto M, Sudhof TC. Mints, Munc18-interacting proteins in synaptic vesicle exocytosis. *J Biol Chem*. 1997;272:31459-31464.
30. Medine CN, Rickman C, Chamberlain LH, Duncan RR. Munc18-1 prevents the formation of ectopic SNARE complexes in living cells. *J Cell Sci*. 2007;120(Pt 24):4407-4415.
31. Burkhardt P, Hattendorf DA, Weis WI, Fasshauer D. Munc18a controls SNARE assembly through its interaction with the syntaxin N-peptide. *EMBO J*. 2008;27:923-933.
32. Deak F, Xu Y, Chang WP, et al. Munc18-1 binding to the neuronal SNARE complex controls synaptic vesicle priming. *J Cell Biol*. 2009;184:751-764.
33. Dulubova I, Khvotchev M, Liu S, Huryeva I, Sudhof TC, Rizo J. Munc18-1 binds directly to the neuronal SNARE complex. *Proc Natl Acad Sci U S A*. 2007;104:2697-2702.
34. Hata Y, Slaughter CA, Sudhof TC. Synaptic vesicle fusion complex contains unc-18 homologue bound to syntaxin. *Nature*. 1993;366:347-351.
35. Khvotchev M, Dulubova I, Sun J, Dai H, Rizo J, Sudhof TC. Dual modes of Munc18-1/SNARE interactions are coupled by functionally critical binding to syntaxin-1 N terminus. *J Neurosci*. 2007;27:12147-12155.
36. Ma C, Li W, Xu Y, Rizo J. Munc13 mediates the transition from the closed syntaxin-Munc18 complex to the SNARE complex. *Nat Struct Mol Biol*. 2011;18:542-549.
37. Misura KM, Scheller RH, Weis WI. Three-dimensional structure of the neuronal-Sec1-syntaxin 1a complex. *Nature*. 2000;404:355-362.
38. Rathore SS, Bend EG, Yu H, Hammarlund M, Jorgensen EM, Shen J. Syntaxin N-terminal peptide motif is an initiation factor for the assembly of the SNARE-Sec1/Munc18 membrane fusion complex. *Proc Natl Acad Sci U S A*. 2010;107:22399-22406.
39. Rickman C, Medine CN, Bergmann A, Duncan RR. Functionally and spatially distinct modes of munc18-syntaxin 1 interaction. *J Biol Chem*. 2007;282:12097-12103.
40. Shen J, Tareste DC, Paumet F, Rothman JE, Melia TJ. Selective activation of cognate SNAREpins by Sec1/Munc18 proteins. *Cell*. 2007;128:183-195.
41. Jiao J, He M, Port SA, et al. Munc18-1 catalyzes neuronal SNARE assembly by templating SNARE association. *Elife*. 2018;7:e41771.
42. Parisotto D, Pfau M, Scheutzow A, et al. An extended helical conformation in domain 3a of Munc18-1 provides a template for SNARE (soluble N-ethylmaleimide-sensitive factor attachment protein receptor) complex assembly. *J Biol Chem*. 2014;289: 9639-9650.
43. Sitarska E, Xu J, Park S, et al. Autoinhibition of Munc18-1 modulates synaptobrevin binding and helps to enable Munc13-dependent regulation of membrane fusion. *Elife*. 2017;6:e24278.
44. Wang S, Li Y, Gong J, et al. Munc18 and Munc13 serve as a functional template to orchestrate neuronal SNARE complex assembly. *Nat Commun*. 2019;10:69.
45. Groffen AJ, Martens S, Diez Arazola R, et al. Doc2b is a high-affinity Ca2 + sensor for spontaneous neurotransmitter release. *Science*. 2010;327:1614-1618.
46. Groffen AJ, Brian EC, Dudok JJ, Kampmeijer J, Toonen RF, Verhage M. Ca(2+)-induced recruitment of the secretory vesicle protein DOC2B to the target membrane. *J Biol Chem*. 2004;279: 23740-23747.
47. Groffen AJ, Friedrich R, Brian EC, Ashery U, Verhage M. DOC2A and DOC2B are sensors for neuronal activity with unique calcium-dependent and kinetic properties. *J Neurochem*. 2006; 97:818-833.
48. Pang ZP, Bacaj T, Yang X, Zhou P, Xu W, Sudhof TC. Doc2 supports spontaneous synaptic transmission by a Ca(2+)-independent mechanism. *Neuron*. 2011;70:244-251.
49. Yao J, Gaffaney JD, Kwon SE, Chapman ER. Doc2 is a Ca2+ sensor required for asynchronous neurotransmitter release. *Cell*. 2011; 147:666-677.
50. Sakaguchi G, Manabe T, Kobayashi K, et al. Doc2alpha is an activity-dependent modulator of excitatory synaptic transmission. *Eur J Neurosci*. 1999;11:4262-4268.

51. Xue R, Ruhl DA, Briguglio JS, Figueroa AG, Pearce RA, Chapman ER. Doc2-mediated superpriming supports synaptic augmentation. *Proc Natl Acad Sci U S A*. 2018;115:E5605-E5613.
52. Biederer T, Sudhof TC. Mints as adaptors. Direct binding to neurexins and recruitment of munc18. *J Biol Chem*. 2000;275:39803-39806.
53. Fukuda M. Regulation of secretory vesicle traffic by Rab small GTPases. *Cell Mol Life Sci*. 2008;65:2801-2813.
54. Nonet ML, Staunton JE, Kilgard MP, et al. Caenorhabditis elegans rab-3 mutant synapses exhibit impaired function and are partially depleted of vesicles. *J Neurosci*. 1997;17:8061-8073.
55. Schluter OM, Schmitz F, Jahn R, Rosenmund C, Sudhof TC. A complete genetic analysis of neuronal Rab3 function. *J Neurosci*. 2004;24:6629-6637.
56. Toonen RF, de Vries KJ, Zalm R, Sudhof TC, Verhage M. Munc18-1 stabilizes syntaxin 1, but is not essential for syntaxin 1 targeting and SNARE complex formation. *J Neurochem*. 2005;93:1393-1400.
57. Chai YJ, Sierecki E, Tomatis VM, et al. Munc18-1 is a molecular chaperone for alpha-synuclein, controlling its self-replicating aggregation. *J Cell Biol*. 2016;214:705-718.
58. Sakai K, Miyazaki J. A transgenic mouse line that retains Cre recombinase activity in mature oocytes irrespective of the cre transgene transmission. *Biochem Biophys Res Commun*. 1997;237:318-324.
59. Burré J, Sharma M, Tsetsenis T, Buchman V, Etherton MR, Sudhof TC. Alpha-synuclein promotes SNARE-complex assembly in vivo and in vitro. *Science*. 2010;329:1663-1667.
60. Burré J, Beckhaus T, Schagger H, et al. Analysis of the synaptic vesicle proteome using three gel-based protein separation techniques. *Proteomics*. 2006;6:6250-6262.
61. Heeroma JH, Roelandse M, Wierda K, et al. Trophic support delays but does not prevent cell-intrinsic degeneration of neurons deficient for Munc18-1. *Eur J Neurosci*. 2004;20:623-634.
62. Santos TC, Wierda K, Broeke JH, Toonen RF, Verhage M. Early Golgi abnormalities and neurodegeneration upon loss of presynaptic proteins Munc18-1, syntaxin-1, or SNAP-25. *J Neurosci*. 2017;37:4525-4539.
63. Abramov D, Guiberson NGL, Daab A, et al. Targeted stabilization of Munc18-1 function via pharmacological chaperones. *EMBO Mol Med*. 2021;13:e12354.
64. Martin S, Papadopulos A, Tomatis VM, et al. Increased polyubiquitination and proteasomal degradation of a Munc18-1 disease-linked mutant causes temperature-sensitive defect in exocytosis. *Cell Rep*. 2014;9:206-218.
65. Vardar G, Chang S, Arancillo M, Wu YJ, Trimbuch T, Rosenmund C. Distinct functions of syntaxin-1 in neuronal maintenance, synaptic vesicle docking, and fusion in mouse neurons. *J Neurosci*. 2016;36:7911-7924.
66. Patzke C, Han Y, Covy J, et al. Analysis of conditional heterozygous STXBP1 mutations in human neurons. *J Clin Invest*. 2015;125:3560-3571.
67. Yamashita S, Chiyonobu T, Yoshida M, et al. Mislocalization of syntaxin-1 and impaired neurite growth observed in a human iPSC model for STXBP1-related epileptic encephalopathy. *Epilepsia*. 2016;57:e81-6.
68. Courtney NA, Briguglio JS, Bradberry MM, Greer C, Chapman ER. Excitatory and inhibitory neurons utilize different Ca(2+) sensors and sources to regulate spontaneous release. *Neuron*. 2018;98:977-991 e5.
69. Toonen RF, Wierda K, Sons MS, et al. Munc18-1 expression levels control synapse recovery by regulating readily releasable pool size. *Proc Natl Acad Sci U S A*. 2006;103:18332-18337.
70. McLeod F, Dimtsi A, Marshall AC, et al. Altered synaptic connectivity in an in vitro human model of STXBP1 encephalopathy. *Brain*. 2023;146:850-857.
71. Wu MN, Littleton JT, Bhat MA, Prokop A, Bellen HJ. ROP, the Drosophila Sec1 homolog, interacts with syntaxin and regulates neurotransmitter release in a dosage-dependent manner. *EMBO J*. 1998;17:127-139.
72. Xue R, Gaffaney JD, Chapman ER. Structural elements that underlie Doc2beta function during asynchronous synaptic transmission. *Proc Natl Acad Sci U S A*. 2015;112:E4316-25.
73. Wu Z, Kusick GF, Berns MMM, et al. Synaptotagmin 7 transiently docks synaptic vesicles to support facilitation and Doc2α-triggered asynchronous release. *bioRxiv*. [Preprint] https://doi.org/10.1101/2022.04.21.489101
74. van Berkel AA, Lammertse HCA, Öttl M, et al. Reduced MUNC18-1 levels, synaptic proteome changes, and altered network activity in STXBP1-related disorder patient neurons. *Biol Psychiatry*. 2023;4:284-298.
75. Granseth B, Odermatt B, Royle SJ, Lagnado L. Clathrin-mediated endocytosis is the dominant mechanism of vesicle retrieval at hippocampal synapses. *Neuron*. 2006;51:773-786.
76. Miesenbock G, De Angelis DA, Rothman JE. Visualizing secretion and synaptic transmission with pH-sensitive green fluorescent proteins. *Nature*. 1998;394:192-195.
77. Sankaranarayanan S, Ryan TA. Real-time measurements of vesicle-SNARE recycling in synapses of the central nervous system. *Nat Cell Biol*. 2000;2:197-204.
78. Riordan JD, Nadeau JH. From peas to disease: Modifier genes, network resilience, and the genetics of health. *Am J Hum Genet*. 2017;101:177-191.
79. Alliance of Genome Resources. Accessed 10 November 2023. https://www.alliancegenome.org/gene/HGNC:2986, https://www.alliancegenomeorg/gene/HGNC:2985
80. EMBL-EBI. GWAS Catalog. Accessed 10 November 2023. https://www.ebi.ac.uk/gwas/genes/DOC2B, https://www.ebi.ac.uk/gwas/genes/DOC2A
81. NLM-NCBI-NIH. ClinVar. Accessed 10 November 2023. https://www.ncbi.nlm.nih.gov/clinvar
82. EMBL-EBI. Unitprot. Accessed 10 November 2023. https://www.uniprot.org/uniprotkb/Q14184/variant-viewer
83. Chen W, Cai ZL, Chao ES, et al. Stxbp1/Munc18-1 haploinsufficiency impairs inhibition and mediates key neurological features of STXBP1 encephalopathy. *Elife*. 2020;9:e48705.
84. Ramirez DMO, Crawford DC, Chanaday NL, Trauterman B, Monteggia LM, Kavalali ET. Loss of doc2-dependent spontaneous neurotransmission augments glutamatergic synaptic strength. *J Neurosci*. 2017;37:6224-6230.
85. Kaeser PS, Regehr WG. Molecular mechanisms for synchronous, asynchronous, and spontaneous neurotransmitter release. *Annu Rev Physiol*. 2014;76:333-363.
86. Orock A, Logan S, Deak F. Munc18-1 haploinsufficiency impairs learning and memory by reduced synaptic vesicular release in a model of Ohtahara syndrome. *Mol Cell Neurosci*. 2018;88:33-42.